BACHELOR OF SCIENCE

IN

ELECTRICAL AND ELECTRONIC ENGINEERING

Designing of Plasmonic Diode and Frequency Converter and Their Performance Analysis

Mirza Fuad Adnan (112412)

Hasibul Hasan (112478)

Safial Mojnabin (112419)

Department of Electrical and Electronic Engineering

ISLAMIC UNIVERSITY OF TECHNOLOGY (IUT)

A Subsidiary Organ of Organisation of Islamic Cooperation (OIC)

Dhaka, Bangladesh.

November, 2015

ISLAMIC UNIVERSITY OF TECHNOLOGY (IUT)

Designing of Plasmonic Diode and Frequency Converter and Their Performance Analysis

Mirza Fuad Adnan (112412)

Hasibul Hasan (112478)

Safial Mojnabin (112419)

SUPERVISED BY

RAKIBUL HASAN SAGOR
Assistant Professor, EEE
Islamic University of Technology (IUT) (OIC)
Board Bazar, Gazipur
Bangladesh

Declaration of Authorship

We, Mirza Fuad Adnan (112412), Hasibul Hasan (112478) and Safial Mojnabin (112419), declare that this thesis titled, 'Designing of Plasmonic Diode and Frequency Converter and Their Performance Analysis' and the works presented in it are our own. We confirm that:

- This work has been done for the partial fulfillment of the Bachelor of Science in Electrical and Electronic Engineering degree at this university.

- Any part of this thesis has not been submitted anywhere else for obtaining any degree.

- Where we have consulted the published work of others, we have always clearly attributed the sources.

Submitted By:

_____

Mirza Fuad Adnan (112412)

_____

Hasibul Hasan (112478)

_____

Safial Mojnabin (112419)

Designing of Plasmonic Diode and Frequency Converter and Their Performance Analysis

Approved By:

_____

Rakibul Hasan Sagor

Thesis Supervisor,

Assistant Professor,

Department of Electrical and Electronic Engineering,

Islamic University of Technology.

_____

Prof. Dr. Md. Shahid Ullah

Head of the Department,

Department of Electrical and Electronic Engineering,

Islamic University of Technology.

Abstract

Plasmonic devices are becoming more and more popular research interest due to its capability to overcome few of the shortcomings of electronic devices. One of the major advantage offered by the plasmonic devices is its ability to overcome diffraction limit that arises due to miniaturization of the devices. Out of many plasmonic devices, here plasmonic diodes have been designed. The performance of the designed device was also analyzed in terms of transmitted energy. Here, the performance variation with different wavelength of the used signal was observed. The biasing dependency of the ports on the frequency used led to the designing of a frequency converter. The frequency converter was designed to convert the frequency of the used signal and thus bias the diode as required. In both the devices namely, Plasmonic diode and frequency converter, different modification in the structure were also made to optimize the performance of the devices.

Acknowledgements

First and foremost, we offer gratitude to the Almighty Allah (SWT) for giving us the capability to do this work with good health.

We are grateful to our research supervisor, Rakibul Hasan Sagor, for the support and guidance throughout our research at Islamic University of Technology (IUT). He created a nice research environment for which we were able to explore many ideas without constraint. We have gained a wealth of knowledge and experience in science and engineering through his direction that is beyond value to our future endeavor. For all of his efforts as our true mentor, we express our heartfelt gratitude to him.

We would like to thank all the faculty members of the department of EEE, IUT for their inspiration and help.

And last but not the least we are thankful to our family, friends and well-wishers for their support and inspiration. Without them it would never have been possible for us to make it this far.

Contents

10 Conclusion and Future work

List of figures

Abbreviations

ABC   Absorbing Boundary Condition

ADE   Auxiliary Differential Equation

AlAs   Aluminum Arsenide

DMD   Dielectric-Metal-Dielectric

FDTD   Finite Difference Time Domain

GLS   Gallium Lanthanum Sulfide

IR   Infra-Red

LD   Lorentz-Drude

MDM   Metal-Dielectric-Metal

PLRC   Piecewise Linear Recursive Convoluti

PML   Perfectly Matched Layer

SPP   Surface Plasmon Polariton

TE   Transverse Electric

TM   Transverse Magnetic

Chapter 1

Introduction and Background

Plasmonics have become one of the most attractive research interest in present times. Its ability to overcome the diffraction limit has made it such attractive[1-3].This ability has provided three major advantages, namely faster speed of operation, smaller devices, less power consumption. Other probable applications of surface plasmon polariton(SPP) includes sub-wavelength imaging[4, 5], Bragg's reflector[6], bio-sensing[7], meta materials[8] and also can be implemented in solar cells[9, 10].

In modern technologies, the speed requirement of the data processing has come to a certain stage where the speed and time taken for electron movement has become a major concern. To shorten the electron transit times less, the devices need to be miniaturised. The miniaturization of the devices leads to several problems like heat dissipation problem, decrease of noise margin etc. Optical devices solve a lot of problems associated with traditional electronics. Photons travelling on optical fibres or thin film will be used in those optical processors making the system lighter and more compact[11, 12].

At present, the communication system is fully dependent on the optical fibers which offer high bandwidth and low loss than electronic interconnections. The same advantage can be availed if the optical technology is used in computer chips. Also, the optical chips will not require any insulation since photons do not interact with each other, making the system lighter. However, the diffraction limit of light restricts the application of conventional optics in making nanometer scale integrated circuits. According tothe diffraction limit rule, light cannot propagate through aperture that is smaller than half of its wavelength.

Out of all plasmonic devices designed so far, plasmonic diode has versatile use in optical computing, interconnection of systems. Different models of nonlinear diode have been proposed so far out of which following are mentionable- left-handed periodic structures with a Kerr nonlinear defect layer[13], periodically poled Lithium Niobate waveguide[14], photonic crystal fiber, nonlinear photonic crystal and photonic bandgap microcavities[15-19], low symmetry magnetic photonic crystals etc.

While implementing pasmonic diode in circuits, the used frequency can be an issue during the biasing and performance of the designed plasmonic diodes. So, a frequency converter can be used for making the frequency of the used signals suitable for desired purposes. This frequency converter can be also used in the optical fiber communication while implementation of FDMA schemes for multimode fibers.

1.1 Overview of Surface-Plasmon-Polariton

Surface plasmon polaritons are electromagnetic excitations propagating at the interface between a dielectric and a conductor, evanescently confined in the perpendicular direction[2]. These electromagnetic surface waves arise via the coupling of the electromagnetic fields to oscillations of the conductor's electron plasma.

The eigenmodes of an interface between a dielectric and a metal are surface plasmon polaritons (SPPs)[20]. We refer to them as eigenmodes in the sense that they are solutions of Maxwell's equations that can be formulated in the absence of an incident field . On a flat interface between dielectric and metal half-spaces with dielectric constants ε_d and ε_m, respectively, SPPs are transverse magnetic (TM) plane waves propagating along the interface. Assuming the interface is normal to z and the SPPs propagate along the x direction, the SPP wave vector k_x is related to the optical frequency through the dispersion relation[21].

$$k_x = k_o\sqrt{\epsilon_d\epsilon_m/(\epsilon_d + \epsilon_m)} \qquad (1.1)$$

where, $k_0 = \frac{\omega}{c}$ is the free-space wave vector. We take ω to be real and allow k_x to be complex, since our main interest is in stationary monochromatic SPP fields in a finite area [22]. The details of SPP has been discussed in Chapter 2.

1.2 Literature Review

Plasmonic devices specially the plasmonic diodes have been a great filed of interest over the recent years. A number of researches have been carried out throughout recent years on the same topic. However, there's still huge scope for the researches in this field. Here in this section of literature review, focus have been made on the literature review of the published works on SPP propagation analysis through different structures with different geometries and most importantly, on plasmonic diodes and also frequency converters.

The parameters of several metals have been reported to our knowledge. Jin et al.[23] determined the modified Debye model parameters for gold which are applicable in the wavelength range of 550-950 nm. Krug et al. [24] reported the gold parameters that are applicable in the wavelength range of 700-1000 nm. W.H.P. Pernice et al.[25] extracted the parameters for Nickel using Lorentz-Drude model. A.D. Rakic et al.[26] reported the parameters for Nickel, Palladium, Titanium and 8 other metals using Lorentz-Drude and Brendel-Bormann Model. M.A. Ordal et al.[27] extracted the parameters for fourteen metals in the infrared and far-infrared range.

Bends, splitters and recombinations are inevitable parts of the optoelectronic devices. Several works on the analysis of SPP propagation in these shapes have been reported to our knowledge. G. Veronis et al. [28] showed that bends and splitters can be designed over a wide frequency range without much loss by keeping centre layer thickness small compared to wavelength. H. Gao et al.[29] investigated the propagation and combination of SPP in Y-shaped channels. B. Wang et al.[30] analyzed two structures which consist of splitting and recombination.

The propagation loss of SPP is very high in metal-dielectric-metal configuration of plasmonic waveguide which limits the length of propagation. Even the fabrication related disorders have far less impact on the propagation loss than the losses that occur in metallic layers of the MDM waveguide. This problem can be addressed by using both dielectric and plasmonic waveguide on the same chip. The dielectric waveguide will carry the fundamental optical mode while the plasmonic waveguide will address

the sub-wavelength scale issue. This calls for the need of efficient coupling of optical modes from the dielectric waveguide to the plasmonic waveguide. Therefore, designing efficient nanoplasmonic couplers with different materials and structures can be a pioneering step in miniaturization of the integrated photonic devices. In the past years, several plasmonic couplers have been proposed by different researchers. G. Veronis et. Al.[31] proposed a coupler with multi-section tapers. P. Ginzburg et al.[32] reported a λ/4 coupler to couple optical modes from a 0.5m to 50nm wide plasmonic waveguide. D. Pile et al.[33] presented an adiabatic and a non-adiabatic tapered plasmonic coupler. R. Washleh et al.[34] reported an analysis on nanoplasmonic air-slot coupler and its fabrication steps.

For the designing of plasmonic diodes, metal-dielectric interfaces are very popular. Different types of structures have been proposed till now on this metal-dielectric interfaces. Zhi-Yuan Li proposed all optical diode and also plasmonic attenuation and quasi-phase-matching (QPM) was harnessed to improve its performance greatly. The structure with gratings was introduced by Xiaoyong Hu et al. where the performance analysis in terms of transmittance contrast was done. Also, analysis have been done on the variation of performance of the diode with the change in grating structures and dimensions.

The implementation of frequency conversion due to polarization is yet to be exploited fully. However, some of the properties and behavior regarding the frequency conversion have been analyzed by Zhi-Yuan Li et al.

1.3   Thesis objective:

The main objective of the thesis is to design the plasmonic devices. Here we have proposed a structure that's works like a diode. And in terms of energy the results indicates the authentication of the device. However, more specifically, the objectives are

- To develop a simulation model based on the FDTD method that is capable of simulating the devices.

- To obtain validity of the designed nano structures by measuring the energy through different ports

- To summarize important conclusions from the obtained results and discuss the potential applications.

1.4 Thesis organization

The thesis has been arranged in the following way-

- In Chapter 2, the basic theory of SPP propagation has been described. This chapter introduces the fundamental knowledge and necessary mathematical formulations of SPP propagation at the single and double interface.
- In Chapter 3, the widely used models for modeling metals have been described in detail with necessary derivations. Since SPPs are created due to the coupling of photon energy to the free electrons of metal, modeling metals is one of the key steps for the simulation of SPP propagation.
- Since we have developed our simulation model based on FDTD method, Chapter 4 introduces the fundamentals of the FDTD algorithm for 1D and 2D simulations. The original formulations of Yee do not include the frequency dependent dispersion properties of materials. We have used the ADE based general algorithm for our simulation model which is discussed in Chapter 4. This chapter also discusses about the absorbing boundary condition.
- In chapter 5 modified Debey model, Lorentz model is discussed and also a developed simulation model is established
- In chapter 6 the design of plasmonic diode along with the Ex,Ey,Hz profiles on the Metal-Dielectric-Metal interfaces and the snapshots of Hz field is provided.
- In chapter 7 the validity of the design of the proposed device including the modifications are provided
- In chapter 8 a design of frequency converter is provided
- In chapter 9 the validity of the design of the frequency converter is provided

Chapter 2

SPP Propagation Theory

2.1 Introduction

Surface plasmon polariton (SPP) is an electromagnetic excitation that propagates in a wave like fashion along the planar interface between a metal and a dielectric medium, often vacuum, and whose amplitude decays exponentially with increasing distance into each medium from the interface. Electromagnetic wave propagation is obtained from

the solution of Maxwell's equations in each medium, and the asso-ciated boundary conditions. Maxwell's equations of macroscopic electromagnetism can be written as follows:

From Gauss's Law for the electric field

$$\nabla . D = \rho_{ext} \tag{2.1}$$

From Gauss's Law for the magnetic field

$$\nabla . B = 0 \tag{2.2}$$

From Faraday's Law

$$\nabla \times E = -\frac{\partial B}{\partial t} \tag{2.3}$$

From Ampere's Law

$$\nabla \times H = J_{ext} + \frac{\partial D}{\partial t} \tag{2.4}$$

Here,

E is the electric field vector in volt per meter

D is the electric flux density vector in coulombs per square meter

H is the magnetic field vector in amperes per meter

B is the magnetic flux density vector in webbers per square meter

$_{ext}$ is the charge density

J_{ext} is the current density

The four macroscopic fields can be also linked further via the polarization P and magnetization M by

$$D = \varepsilon_0 E + P \tag{2.5}$$

$$H = \frac{1}{\mu_0} B - M \tag{2.6}$$

Now this equations can be simplified for linear, isotropic, nonmagnetic media as

$$D = \varepsilon_0 \varepsilon_r E \tag{2.7}$$

$$B = \mu_0 \mu_r H \tag{2.8}$$

where,

ε_0 is electric permittivity of vacuum in Farad per meter

μ_0 is the magnetic permeability of vacuum in Henry per meter

ε_r is the relative permittivity

μ_r is the relative permeability

2.2 The EM or Electromagnetic Wave Equation

The EM wave equation which describes the field amplitude in time and space can be derived from Maxwell's equations. The wave equation can be derived by taking curl of Faraday's law

$$\nabla \times \nabla \times E = -\frac{\partial B}{\partial t} \tag{2.9}$$

or,

$$\nabla \times \nabla \times E = \nabla \times (-\mu \frac{\partial H}{\partial t}) \tag{2.10}$$

with the identities $\nabla \times \nabla \times E = \nabla(\nabla.E) - \nabla^2 E$ and $\nabla \times H = \varepsilon \frac{\partial E}{\partial t}$ we can simplify
the above equation as

$$\nabla(\nabla.E) - \nabla^2 E = -\mu\varepsilon \frac{\partial^2 y}{\partial t^2} \tag{2.11}$$

From Gauss's law we can conclude that the divergence of E in a constant permittivity over space is zero. i,e $\nabla.E = 0$

Therefore, the final wave equation for electric field will be

$$\nabla^2 E - \mu\varepsilon \frac{\partial^2 E}{\partial t^2} = 0 \tag{2.12}$$

Similarly the wave equation for magnetic field can be derived as

$$\nabla^2 H - \mu\varepsilon \frac{\partial^2 H}{\partial t^2} = 0 \tag{2.13}$$

So, the general form of wave equation can be written as

$$\nabla^2 U - \frac{1}{v_p^2} \left(\frac{\partial^2 H}{\partial t^2}\right) = 0 \tag{2.14}$$

If the variation of the dielectric profile " is negligible over distance, then we can write

$$\nabla^2 E - \frac{\varepsilon}{C^2} \frac{\partial^2 E}{\partial t^2} = 0 \tag{2.15}$$

Where $C = \frac{1}{\sqrt{\mu_0 \, \varepsilon_0}}$ velocity of light

The solution of wave equation is a harmonic function in time and space. Now if we assume this as a harmonic time dependence of the electric field,

$$E(r,t) = E(r)e^{-j\omega t} \tag{2.16}$$

Therefore we get the Helmholtz equation

$$\nabla^2 E + K_0^2 \varepsilon E = 0 \tag{2.17}$$

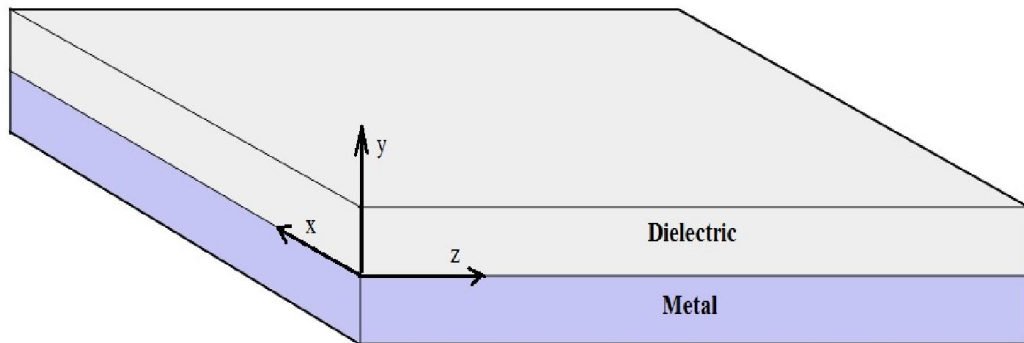where the vector of propagation $K_0 = \frac{\omega}{C}$, in free space

Fig 2.1: Typical planar waveguide geometry. The waves propagate along the x-direction in a cartesian coordinate system

For simplicity let us assume the propagation of wave is along the x-direction of the

Cartesian co-ordinate system and no spatial variation in y-direction. So we can write

$$E(x,y,z) = E(z)e^{j\beta z} \tag{2.18}$$

Where $\beta = K_x$ which is call the propagation constant

Now inserting the value of E the wave equation will be

$$\frac{\partial^2 E(z)}{\partial z^2} + (K_0^2 \varepsilon - \beta^2)E = 0 \tag{2.19}$$

Similarly we can derive the equation for the magnetic field H. The field E and H can be decomposed in cartesian co-ordinate system as

$$E = E_x.\vec{a}_x + E_y.\vec{a}_y + E_z.\vec{a}_z \tag{2.20}$$

$$H = H_x.\vec{a}_x + H_y.\vec{a}_y + H_z.\vec{a}_z \tag{2.21}$$

For Harmonic time dependence $\frac{\partial}{\partial t} = -j\omega$ and by solving the Ampere's law and Faraday's law, we get

$$\frac{\partial E_z}{\partial y} - \frac{\partial E_y}{\partial z} = j\omega\mu_0\, H_x \tag{2.22}$$

$$\frac{\partial E_x}{\partial z} - \frac{\partial E_z}{\partial x} = j\omega\mu_0\, H_y \tag{2.23}$$

$$\frac{\partial E_y}{\partial x} - \frac{\partial E_x}{\partial y} = j\omega\mu_0\, H_z \tag{2.24}$$

$$\frac{\partial Hz}{\partial y} - \frac{\partial H_y}{\partial z} = j\omega\varepsilon_0\, \varepsilon E_x \tag{2.25}$$

$$\frac{\partial Hx}{\partial z} - \frac{\partial H_z}{\partial x} = j\omega\varepsilon_0\, \varepsilon E_y \tag{2.26}$$

$$\frac{\partial Hy}{\partial x} - \frac{\partial H_x}{\partial y} = j\omega\varepsilon_0\, \varepsilon E_z \tag{2.27}$$

As the propagation is in x-direction in the form of $e^{j\beta x}$ which follows $\frac{\partial}{\partial x} = -j\beta$.

The homogeneity in y- direction make $\frac{\partial}{\partial y} = 0$. So the equation will be simplified as

$$-\frac{\partial E_y}{\partial z} = j\omega\mu_0\, H_x \tag{2.28}$$

$$\frac{\partial E_x}{\partial z} - j\beta E_z = j\omega\mu_0\, H_y \tag{2.29}$$

$$jβE_y = jωμ_0 H_z \tag{2.30}$$

$$\frac{∂H_y}{∂z} = jωε_0\, εE_x \tag{2.31}$$

$$\frac{∂Hx}{∂z} - jβH_z = jωε_0\, εE_y \tag{2.32}$$

$$jβH_y = jωε_0\, εE_z \tag{2.33}$$

The solution of the above equation can be characterized by two sets of solution with the polarized characteristics which are, Transverse Magnetic (TM) modes and Transverse Electric (TE) modes. The equations belong to TM modes are

$$E_x = -j\frac{1}{ωε_0\, ε}\frac{∂H_y}{∂z} \tag{2.34}$$

$$E_z = -β\frac{1}{ωε_0\, ε}H_y \tag{2.35}$$

Therefore, the wave equation for TM Polarized wave will be

$$\frac{∂^2H_y}{∂z^2} + (K_0^2 ε - β^2)H_y = 0 \tag{2.36}$$

Similarly the TE polarized equations will be

$$H_x = j\frac{1}{ωμ_0}\frac{∂E_y}{∂z} \tag{2.37}$$

$$H_z = β\frac{1}{ωμ_0}E_y \tag{2.37}$$

And the corresponding TE wave equation will be

$$\frac{∂^2E_y}{∂z^2} + (K_0^2 ε - β^2)E_y = 0 \tag{2.38}$$

2.3   SPP at Single Interface

The simplest configuration of SPP propagation is at single interface, that is in between dielectric, having the positive dielectric constant $ε_2$ and metal, having the negative dielectric constant $ε_1$. For metal the bulk plasmon frquency will be $ω_p$ and the amplitude decays perpendicular to the $z-$ direction.

For the TM solutions in both spaces: metal and dielectric will be for $z > 0$

$$H_z(z) = A_2 e^{j\beta x} e^{-k_2 z} \qquad (2.40)$$
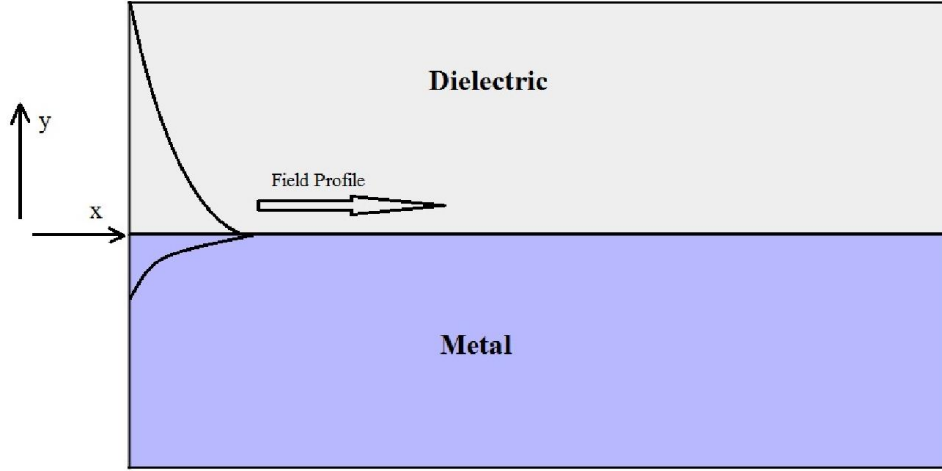
Fig 2.2: SPP at the Single interface.

$$E_x(z) = jA_2 \frac{1}{\omega \varepsilon_0 \varepsilon_2} k_2 e^{j\beta x} e^{-k_2 z} \qquad (2.41)$$

$$E_z(z) = -A_1 \frac{\beta}{\omega \varepsilon_0 \varepsilon_2} e^{j\beta x} e^{-k_2 z} \qquad (2.42)$$

And for $z < 0$

$$H_y(z) = A_1 e^{j\beta x} e^{k_1 z} \qquad (2.43)$$

$$E_x(z) = -jA_1 \frac{1}{\omega \varepsilon_0 \varepsilon_1} k_1 e^{j\beta x} e^{k_1 z} \qquad (2.44)$$

$$E_x(z) = -A_1 \frac{\beta}{\omega \varepsilon_0 \varepsilon_1} e^{j\beta x} e^{-k_1 z} \qquad (2.45)$$

The continuity of H_y and $\varepsilon_i E_z$ at the metal dielectric interface gives $A_1 = A_2$ and

$$\frac{k_2}{k_1} = -\frac{\varepsilon_2}{\varepsilon_1} \qquad (2.46)$$

The surface wave exists at the metal dielectric interface with opposite sign of their real dielectric permittivities. So, we can write

$$k_1^2\varepsilon = \beta^2 - k_0^2\varepsilon_1 \qquad (2.47)$$

$$k_2^2\varepsilon = \beta^2 - k_0^2\varepsilon_2 \qquad (2.48)$$

The dispersion relation of SPPs propagation can be found as

$$\beta = k_0\sqrt{\frac{\varepsilon_1\varepsilon_2}{\varepsilon_1+\varepsilon_2}} \qquad (2.49)$$

The TE surface modes can be expressed as

$$E_y(z) = A_2 e^{j\beta x} e^{-k_2 z} \qquad (2.50)$$

$$H_x(z) = -jA_2 \frac{\beta}{\omega\mu_0} k_2 e^{j\beta x} e^{-k_2 z} \qquad (2.51)$$

$$H_z(z) = -A_2 \frac{\beta}{\omega\mu_0} k_2 e^{j\beta x} e^{-k_2 z} \qquad (2.52)$$

for $z > 0$, and

$$E_y(z) = A_1 e^{j\beta x} e^{-k_1 z} \qquad (2.53)$$

$$H_x(z) = jA_1 \frac{\beta}{\omega\varepsilon_0 \varepsilon_1} k_1 e^{j\beta x} e^{k_1 z} \qquad (2.54)$$

$$H_z(z) = A_1 \frac{\beta}{\omega\varepsilon_0 \varepsilon_1} k_2 e^{j\beta x} e^{k_1 z} \qquad (2.55)$$

for $z < 0$. The continuity of E_y and H_x requires

$$A_1 (k_1 + k_2) = 0 \qquad (2.55)$$

The surface requires that the real part of k_1 and k_2 should be greater than zero for confinement. This will be satisfied if $A_1 = A_2 = 0$. Therefore no surface modes for the TE polarization. SPP only exist for TM mode polarization.

2.4   SPP at Double Interface

Two mostly used double interface configurations of SPP waveguides are: Metal-Dielectric-Metal(MDM) and Dielectric-Metal-Dielectric (DMD). In these cases SPPs are formed on both interfaces. When the distance is shorter than decay distance, it forms

coupled mode of SPP. This coupled mode of propagation can also be sub-divided into even and odd modes, as shown in the figure
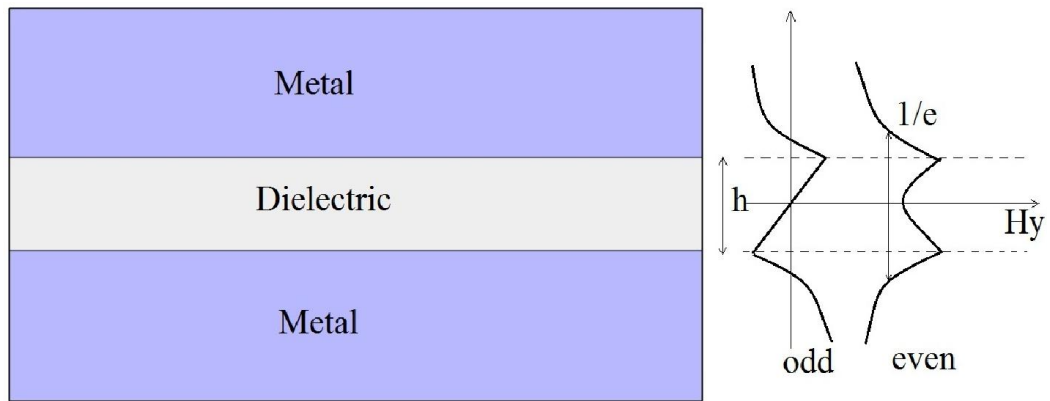
Fig 2.3: SPP at the double interface.

Chapter 3

Material Modeling Within Optical Range

3.1 Introduction

At low frequencies or for long wavelengths metals act as perfect conductors. Since it has zero field, they do not show any dispersive behavior. But at higher frequen-cies such as optical range metals behave as dispersive materials which means that there exists field inside metal. And for the frequencies higher than optical range metals act as dielectrics. Properties of SPPs depend highly on the material re-sponse to light. In this chapter we will be studying about the material supporting SPP, descriptions and derivations of different models for describing the behavior of metal in the presence of light.

Now in presence of an external oscillating electromagnetic field, three vectors can determine the behavior of any material. Such as: D (electrical flux density), E (electric field intensity) and P (polarization density). In frequency domain the corresponding equation will be

$$D(\omega) = \varepsilon(\omega)E(\omega) \tag{3.1}$$

$$P(\omega) = \varepsilon_0 \chi(\omega)E(\omega) \tag{3.2}$$

$$D(\omega) = \varepsilon_0 E(\omega) + P(\omega) \tag{3.3}$$

Combining this two equations we get

$$D(\omega) = \varepsilon_0 E(\omega)(1 + \chi(\omega)) \tag{3.4}$$

Where χ is the electric susceptibility which measures how easily it is polarized in response to an applied electric field, and it is a dimensionless quantity.

Finally the relation between the the permittivity and susceptibility is

$$\varepsilon(\omega) = \varepsilon_0(1 + \chi(\omega)) \qquad (3.5)$$

So the relative permittivity will be

$$\varepsilon_r(\omega) = 1 + \chi(\omega) \qquad (3.5)$$

For linear isotropic materials such as glass this above values become simple. But for a dispersive material, the frequency dependent permittivity and susceptibility should be modeled perfectly for getting the perfect response of the material for certain electromagnetic excitation. Some widely used material models are Drude model, Lorentz model, Debye model and Lorentz-Drude model.

3.2   Different Material Models

3.2.1   The Drude Model

The Drude model of electrical conduction was first developed by Paul Drude. In his model he described the metal as a volume filled with stationary positive ions, immersed in a gas of electrons following the kinetic theory of gases. These electrons are free to move inside the metal without any interaction with each other. The electrons in a metal are subjected to two forces, such as

1. Driving force F_d
2. Damping force F_g

The driving force and the damping force can be expressed as

$$F_d = qE = -eE \tag{3.7}$$

$$F_g = -\Gamma v \tag{3.8}$$

As the two forces are opposite to each other, the resultant force will be

$$F = F_d - F_g \tag{3.9}$$

From Newton's first law of motion we can write

$$mr'' = -eE + \Gamma r' \tag{3.10}$$

where,
m is the mass of an electron

Γ is the damping constant in Newton second per meter

r is the displacement in meter.

v is the velocity of the electron .

q is the electrons charge.

The prime indicates differentiation order with respect to time

For time harmonic electric field and time harmonic displacement the equation will be

$$E(t) = E_0 e^{-j\omega t} \Leftrightarrow E(\omega) \tag{3.11}$$
$$r(t) = R_0 e^{-j\omega t} \Leftrightarrow R(\omega) \tag{3.12}$$

From equaion 3.10 the frequency domain form will be
$$mR''(\omega) - \Gamma mR'(\omega) + eE(\omega) = 0 \tag{3.13}$$

The derivatives of frequency domain will give

$$-m\omega^2 R''(\omega) + j\omega\Gamma mR'(\omega) + eE(\omega) = 0 \tag{3.14}$$

Simplifying the above equation, the displacement R will give

$$R(\omega) = \frac{-e}{m(j\Gamma\omega - \omega^2)} E(\omega) \tag{3.15}$$

The polarization for n number of electrons will be

$$P(\omega) = -neR(\omega) \tag{3.16}$$

Or,

$$P(\omega) = \frac{e^2 n}{m(j\Gamma\omega - \omega^2)} E(\omega) \tag{3.17}$$

An expression for the susceptibility can also be obtained from the above equation and that will be

$$\frac{P(\omega)}{\varepsilon_0 E(\omega)} = \frac{e^2 n}{\varepsilon_0 m(j\Gamma\omega - \omega^2)} = \chi(\omega) \qquad (3.18)$$

Now substituting this value in equation 3.6 we get

$$\varepsilon_r(\omega) = 1 + \frac{e^2 n}{\varepsilon_0 m(j\Gamma\omega - \omega^2)} \qquad (3.19)$$

if we consider ω_p as the plasma frequency that will provide

$$\omega_p^2 = \frac{e^2 n}{\varepsilon_0 m} \qquad (3.20)$$

So, the frequency dependent flux density will be

$$D(\omega) = \varepsilon_0 (1 + \frac{\omega_p^2}{(j\Gamma\omega - \omega^2)}) E(\omega) \qquad (3.21)$$

For low frequency, the term $\Gamma\omega \ll 1$ therefore, the dispersive relation can be reduced to

$$D(\omega) = \varepsilon_0 (1 - \frac{\omega_p^2}{(\omega^2)}) E(\omega) \qquad (3.22)$$

3.2.2 The Lorentz Model

The Lorentz model gives a simpler picture of the atom. The model is a very useful tool to visualize atom-field interaction. In this model, Lorentz modeled an atom as a mass (nucleus) connected to another smaller mass (electron). However, electrons in the Lorentz model do not move freely inside the metal instead, they are bound to atoms. So, there is a restoring force acting between them which can be denoted by F_r
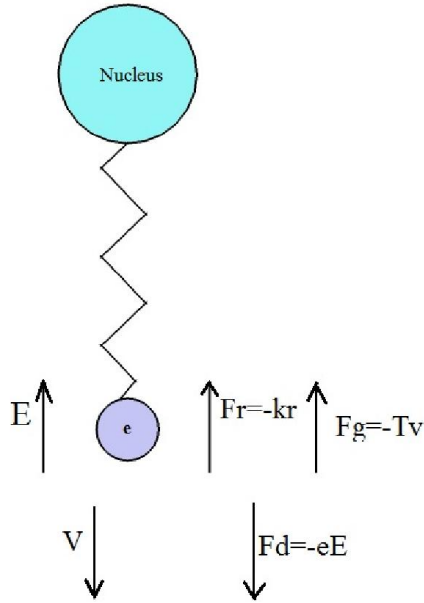
Fig 3.2: Lorentz model

The restoring force can be written as

$$F_r = -kr \tag{3.22}$$

where k is the spring constant in Newtons per meter.

Similarly from the law of motion we can say that

$$mr'' + \Gamma m r'(\omega) + mkr + eE = 0 \tag{3.23}$$

In frequency domain the above equation will be

$$R(\omega)(m\omega_0^2 + j\omega\Gamma m - m\omega^2 - eE(\omega) = 0 \tag{3.24}$$

Considering the natural frequency $\omega_0 = \sqrt{\dfrac{k}{m}}$ we get

$$R(\omega) = \frac{-e}{m(\omega_0^2 + j\omega\Gamma - \omega^2)} E(\omega) \tag{3.25}$$

Therefore the susceptibility can be found as

$$\frac{P(\omega)}{\varepsilon_0 E(\omega)} = \frac{e^2 n}{\varepsilon_0 m(\omega_0^2 + j\omega\Gamma - \omega^2)} = \chi(\omega) \tag{3.26}$$

So from the equation 3.4 the expression for D can be expressed in frequency domain as

$$D(\omega) = \varepsilon_0 (1 + \frac{\omega_p^2}{\omega_0^2 + j\omega\Gamma - \omega^2}) E(\omega) \qquad (3.27)$$

3.2.3 The Lorentz-Drude Model

In the Lorentz-Drude (LD) model, which is the most general form when an EM field is applied to a metal, the electrons of two types oscillate inside the metal, and they contribute to the permittivity. The free electrons contribute a permittivity of the Drude model, and the bound electrons contribute a permittivity of the Lorentz model. The permittivity in the LD model is given by

$$\varepsilon = \varepsilon_{free} + \varepsilon_{bound} \qquad (3.29)$$

Where

$$\varepsilon_{free} = 1 + \frac{\omega_p}{(j\Gamma\omega - \omega^2)} \qquad (3.30)$$

$$\varepsilon_{bound} = \frac{\omega_p}{\omega_0 + j\omega\Gamma - \omega^2} \qquad (3.31)$$

Therefore combining both the model together the electric field density D in fre-quency domain will be

$$D(\omega) = \varepsilon_0 (1 + \frac{\omega_p}{j\Gamma\omega - \omega^2} + \frac{\omega_p^2}{\omega_0^2 + j\omega\Gamma - \omega^2}) E(\omega) \qquad (3.32)$$

The above relation is known as the Lorentz-Drude model.

3.2.4 The Debye Model

The Debye model was first developed by Peter Debye in the year 1912. According to the Debye model,materials are made of electric dipoles, so that, when an electric field is applied, these dipoles follow the behavior of the applied field with some relaxation time. If the electric field is oscillating at a slow frequency, then the polarization will be strong. On the other hand, a fast oscillating field means low polarization. From another point of view, materials with long relaxation times have low polarization or no polarization at all, and materials with short relaxation times have strong polarization.

Metals are known to have very short relaxation times. Thus, polarization in metals is strong. If a DC electric field is applied to a dielectric, the polarization takes some time to follow the electric field. At steady state, it will be

$$P(t) = P_\infty (1 - e^{-t/\tau}) \tag{3.33}$$

where $P(t)$ is the instantaneous polarization

P_∞ is the polarization in the steady state is the time constant.

The derivative of the above equation will be

$$\frac{dP(t)}{dt} = \frac{1}{\tau} P_\infty e^{-t/\tau} \tag{3.34}$$

Now combining both the equations we get

$$P(t) = P_\infty - \tau \frac{dP(t)}{dt} \tag{3.35}$$

As $P_\infty = \varepsilon_0 (\varepsilon - 1) E(t)$ so the equation will be reduced to

$$P(t) = \varepsilon_0 (\varepsilon - 1) E(t) - \tau \frac{dP(t)}{dt} \tag{3.36}$$

or,

$$\varepsilon_0 (\varepsilon - 1) E(t) = P(t) + \tau \frac{dP(t)}{dt} \tag{3.37}$$

In frequency domain the equation will be

$$\varepsilon_0 (\varepsilon - 1) E(\omega) = P(\varepsilon) + j\omega\tau P(\omega) \tag{3.38}$$

Or,

$$P(\omega) = \frac{\varepsilon_0 (\varepsilon - 1)}{1 + j\omega\tau} E(\omega) \tag{3.39}$$

The susceptibility can be expressed as

$$\frac{(\varepsilon - 1)}{1 + j\omega\tau} = \frac{P(\omega)}{\varepsilon_0 E(\omega)} = \chi(\omega) \tag{3.40}$$

The relative permittivity will be

$$\varepsilon_0(\omega) = \frac{(\varepsilon - 1)}{1 + j\omega\tau} + 1 = 1 + \chi(\omega) \tag{3.41}$$

For the permittivity function to fit in the range from 0 frequency to infinity frequency, the boundary conditions are $\varepsilon_r(0) = \varepsilon_s(0)$ and $\varepsilon_r(\infty) = \varepsilon_\infty(0)$

So,

$$\varepsilon(\omega) = \varepsilon_\infty + \frac{(\varepsilon_s - \varepsilon_\infty)}{1 + j\omega\tau} \tag{3.42}$$

To take into account the material losses that SPPs encounter, another term is added with

the permittivity of metal. So the above equation can be expanded to

$$\varepsilon(\omega) = \varepsilon_\infty + \frac{(\varepsilon_s - \varepsilon_\infty)}{1 + j\omega\tau} - j\frac{\sigma}{\omega\varepsilon_0} \tag{3.43}$$

In real and imaginary term the Debay model is

$$\varepsilon_r(\omega) = \varepsilon'(\omega) - j\varepsilon''(\omega) \tag{3.44}$$

Where-

$$\varepsilon'(\omega) = \varepsilon_\infty + \frac{(\varepsilon_s - \varepsilon_\infty)\omega\tau}{1 + j\omega^2 r^2} \tag{3.45}$$

$$\varepsilon''(\omega) = \varepsilon_\infty + \frac{(\varepsilon_s - \varepsilon_\infty)\omega\tau}{1 + j\omega^2 r^2} + \frac{\sigma}{\omega\varepsilon_0} \tag{3.46}$$

3.3   Material Dispersion

Dispersion can be defined as the variation of the propagating waves wavelength with frequency. It is also sometimes defined as the variation of propagating waves wave number $k = \frac{2\pi}{\lambda}$ with angular frequency $\omega = 2\pi f$. So the one dimensional wave equation will be

$$\frac{\partial^2 u}{\partial t^2} = v^2 \frac{\partial^2 u}{\partial x^2} \tag{3.47}$$

Where,
$$v^2 = \frac{1}{\varepsilon\mu}$$
The solution of the above wave equation can be written in phasor form as

$$u(x,t) = e^{j(\omega t - kx)} \tag{3.48}$$

Now putting this value in the wave equation we get

$$(j\omega)^2 e^{j(\omega t - kx)} = v^2(-jk)^2 e^{j(\omega t - kx)} \tag{3.49}$$

Finally from this equation we get

$$k = \pm\frac{\omega}{v} \tag{3.50}$$

The + sign is for -x directed wave propagation and - sign is for +x directed wave propagation. The magnetic flux density and electric flux density for dispersive medium

are-

$$D(\omega) = \varepsilon(\omega)E \hspace{4cm} (3.51)$$

$$B(\omega) = \mu(\omega)H \hspace{4cm} (3.52)$$

Here both $\varepsilon(\omega)$ and $\mu(\omega)$ are frequency dependent functions.

Chapter 4

Overview of Finite-Difference Time-Domain Method

4.1   The Yee Algorithm

The algorithm used in FDTD simulations is known as the Yee algorithm. The original proposal was intended for homogeneous, isotropic and lossless media based on discretizing the volume into cells in Cartesian coordinates. The Yee algorithm solves for both electric and magnetic fields using the coupled Maxwell's time-dependent curl equations, rather than solving for the electric field alone (or the magnetic field alone) with a wave equation.

The method begins with two of Maxwell's equations:

$$D\frac{\partial \vec{H}}{\partial t} = -\frac{1}{\mu}\nabla \times \vec{E} \tag{4.1}$$

$$D\frac{\partial \vec{E}}{\partial t} = \frac{1}{\varepsilon}\nabla \times \vec{H} \tag{4.2}$$

The electric and magnetic fields are three dimensional vectors. Each equation can be converted into three coupled scalar first order differential equations. The derivatives are both in space and time. The curl operations of equations 4.1 and equation 4.2 yields the following six equations in Cartesian coordinates

$$\frac{\partial E_z}{\partial y} - \frac{\partial E_y}{\partial z} = \mu\frac{\partial H_x}{\partial t} \tag{4.3}$$

$$\frac{\partial E_x}{\partial z} - \frac{\partial E_z}{\partial x} = \mu\frac{\partial H_z}{\partial t} \tag{4.4}$$

$$\frac{\partial E_y}{\partial x} - \frac{\partial E_x}{\partial y} = \mu\frac{\partial H_z}{\partial t} \tag{4.5}$$

$$\frac{\partial Hz}{\partial y} - \frac{\partial H_y}{\partial z} = \varepsilon\frac{\partial E_x}{\partial t} \tag{4.6}$$

$$\frac{\partial Hx}{\partial z} - \frac{\partial H_z}{\partial x} = \varepsilon \frac{\partial E_y}{\partial t} \qquad (4.7)$$

$$\frac{\partial Hy}{\partial x} - \frac{\partial H_x}{\partial y} = \varepsilon \frac{\partial E_z}{\partial t} \qquad (4.8)$$

Then the scalar differential equations are converted into difference equations. In order to do that, discretization is required for both space and time. For space discretization, Yee visualized the field components arranged within a unit cell (voxel). The electric field components are stored on the corresponding cell edges, while the magnetic field components are stored on the corresponding face centers. The fields are located in a way where each E component is surrounded by four

H components and vice versa, which leads to a spatially coupled system of field circulations corresponding to the law of Faraday and Ampere. The figure 4.1 shows the Yee's spatial grid.

Considering a two dimensional TM (Transverse Magnetic) polarized field case,

$$\frac{\partial E_x}{\partial t} = \frac{1}{\varepsilon} \frac{\partial H_z}{\partial y} \qquad (4.9)$$

$$\frac{\partial E_y}{\partial t} = \frac{1}{\varepsilon} \frac{\partial H_z}{\partial x} \qquad (4.10)$$

$$\frac{\partial H_z}{\partial t} = \frac{1}{\mu} \left(\frac{\partial E_x}{\partial y} - \frac{\partial E_y}{\partial x} \right) \qquad (4.11)$$

Central difference approximation is applied in each of the equations 4.9, 4.10 and 4.11 which finally conclude in a spatial scalar difference equations in 4.12, 4.13 and 4.14.
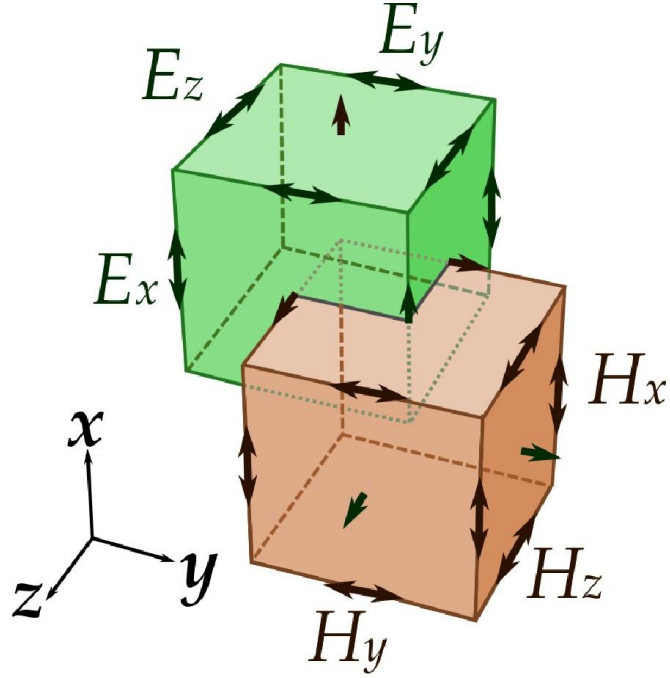
Fig 4.1: Yee's spatial grid.

$$\frac{\partial E_x}{\partial t} = \frac{1}{\varepsilon}\frac{H_z(i,j)-H_z(i,j-1)}{\Delta y} \tag{4.12}$$

$$\frac{\partial E_y}{\partial t} = \frac{1}{\varepsilon}\frac{H_z(i,j)-H_z(i-1,j)}{\Delta x} \tag{4.13}$$

$$\frac{\partial H_z}{\partial t} = \frac{1}{\mu}\left(\frac{E_x(i,j+1)-E_x(i,j)}{\Delta y} - \frac{E_y(i+1,j)-E_y(i-1,j)}{\Delta x}\right) \tag{4.14}$$

In order to consider the time derivatives, the time axis is to be considered as shown in the figure. The Electric and Magnetic field are mapped half a step apart along the time axis. Again applying the central difference approximation the equations 4.12, 4.13 and 4.14 become:

$$\frac{E_x^{n+1}\left(i+\frac{1}{2},j\right)-E_x^n(i+\frac{1}{2},j)}{\Delta t} = \frac{1}{\varepsilon}\frac{H_z^{n+\frac{1}{2}}\left(i+\frac{1}{2},j\right)-H_z^{n+\frac{1}{2}}(i+\frac{1}{2},j-\frac{1}{2})}{\Delta y}$$

$$\frac{E_y^{n+1}\left(i,j+\frac{1}{2}\right)-E_y^n(i,j+\frac{1}{2})}{\Delta t} = -\frac{1}{\varepsilon}\frac{H_z^{n+\frac{1}{2}}\left(i+\frac{1}{2},j+\frac{1}{2}\right)-H_z^{n+\frac{1}{2}}(i-\frac{1}{2},j+\frac{1}{2})}{\Delta y}$$

$$\frac{H_z^{n+\frac{1}{2}}\left(i+\frac{1}{2},j+\frac{1}{2}\right)-H_z^{n-\frac{1}{2}}\left(i+\frac{1}{2},j+\frac{1}{2}\right)}{\Delta t} = -\frac{1}{\mu}\left(\frac{E_x^{n+1}\left(i+\frac{1}{2},j+1\right)-E_x^n\left(i+\frac{1}{2},j\right)}{\Delta y} - \frac{E_y^n\left(i+1,j+\frac{1}{2}\right)-E_y^n\left(i,j+\frac{1}{2}\right)}{\Delta x}\right)$$

Each field component depends on the field of previous time step itself and the surrounding component in Yee's algorithm.
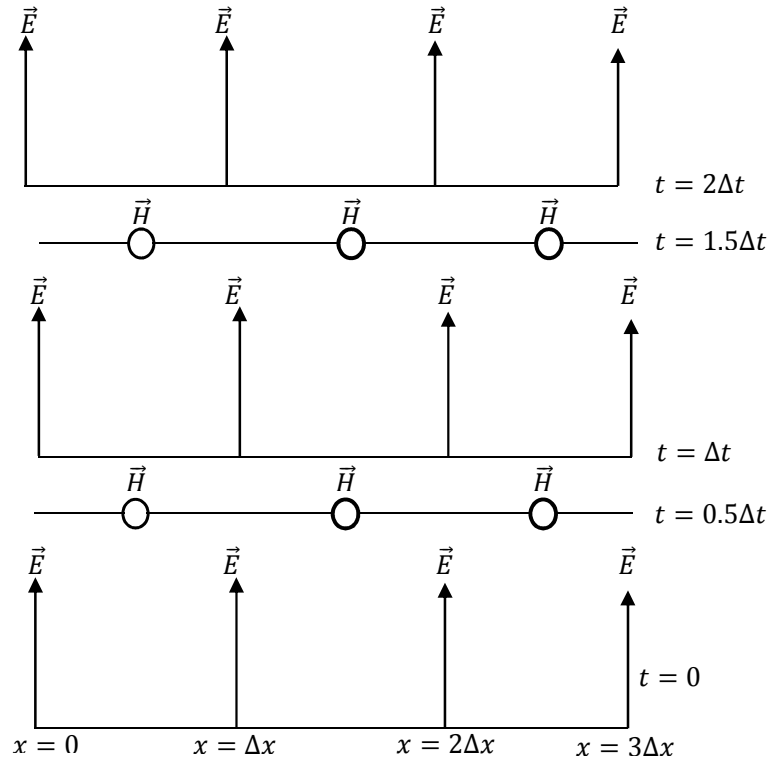

Fig 4.2: The temporal scheme of FDTD method.

Numerical stability of the Yee algorithm is required to be ensured. In an unstable algorithm the computed magnitude of electric and magnetic field components will gradually increase without limit with the progression of simulation. To guarantee numerical stability, the EM field's propagation should not be faster than the al-lowed limit which is imposed by the phase velocity within the material. This is done by limiting time step Δt using the Courant-Friedrichs-Lewy criterion for the general Yee FDTD grid as follows:

$$\Delta t \leq \left\{ \frac{1}{v_p \sqrt{\frac{1}{(\Delta x)^2} + \frac{1}{(\Delta y)^2} + \frac{1}{(\Delta z)^2}}} \right\} \qquad (4.15)$$

where Δx, Δy and Δz indicate the spatial Cartesian grid increments.

4.2   Absorbing Boundary Condition (ABC)

In FDTD method, a space of theoretically infinite extent with a finite compu-tational cell is simulated due to limited computer resources. The boundary is said to be ideally absorbing, without any non-physical reflection back to the re-gion. To accomplish this, a number of boundary conditions such as Berenger's perfectly matched layer (PML), have been proposed. An artificial layer surrounds the computational domain so that most of the outgoing waves are absorbed. The electromagnetic fields are made to attenuate rapidly until they become equal to zero, so that they do not produce any reflections.

4.3   Material Dispersion in FDTD

The material is said to be dispersive when the permittivity and permeability of a material are functions of frequency. In reality the assumption of constant rel-ative permittivity is not absolutely correct. Because by doing so, instantaneous polarization of charge within a material is being assumed. In order to exploit the realistic wave propagation, dispersive FDTD techniques become necessary. The existing FDTD based algorithms for the analysis of material dispersion can be categorized into three types:

1) the auxiliary differential equation (ADE),
2) the Z-transform methods, and
   3) methods base on discrete convolution of the dispersion relation or the recursive convolution (RC) method [35].

We will highlight on the ADE dispersive FDTD method as we have applied in material modeling. The other methods will also be briefly discussed.

4.3.1   The Auxiliary Differential Equation(ADE)

Taflove introduced the auxiliary differential equation to the FDTD modeling in order to integrate the dispersion relation into the model. The dispersion relation is converted from frequency domain to time domain through Fourier transform in the basic step of the procedure. The Fourier transform results in a relationship between the new E field value and the previous E and D values, which can be added to the algorithm to update the E fields. The new algorithm with ADE becomes

$$\frac{\partial}{\partial t} H_z = -\frac{1}{\mu} \left(\frac{\partial E_x}{\partial y} - \frac{\partial E_y}{\partial x} \right) \tag{4.16}$$

$$\frac{\partial}{\partial t} D_x = \frac{\partial H_z}{\partial y} \tag{4.17}$$

In order to get the function relating D to E in a dispersive medium, we start with

$$D(\omega) = \varepsilon_0 \frac{\sigma}{j\omega} E(\omega) \tag{4.18}$$

Multiplying by $j\omega$

$$j\omega D(\omega) = \varepsilon_0 \sigma E(\omega) \tag{4.19}$$

Applying the Fourier transform in equation 4.19

$$\frac{d}{dt} D(t) = \varepsilon_0 \sigma E(t) \tag{4.20}$$

Discretizing equation 4.20 equation using forward difference method

$$\frac{D^n - D^{n-1}}{\Delta t} = \varepsilon_0 \sigma E(t) \tag{4.21}$$

Finally solving for E, we find the update equation

$$E^n = \frac{D^n - D^{n-1}}{\varepsilon_0 \sigma \Delta t} \tag{4.22}$$

4.3.2 The Z-transform Methods

The Z-transform is a faster method compared to ADE method. Sullivan used the Z-transform method for the first time in order to introduce the dispersion relation into the FDTD algorithm.

The Z-transform of the equation

$$D(\omega) = \varepsilon(\omega)E(\omega) \tag{4.23}$$

is -

$$D(z) = \varepsilon(z)\Delta t E(z) \tag{4.24}$$

—

where $\varepsilon(z)$ is the z-transform of $\varepsilon(\omega)$ and is the sampling period. As already done in ODE, let us consider the material dispersion as $\frac{\sigma}{j\omega}$, the relation between D and E is given by

$$D(\omega) = \frac{\sigma\varepsilon_0}{1-z^{-1}}\Delta t E(z) \tag{4.25}$$

Multiplying by $(1 - z^{-1})$, we find

$$D(z)(1 - z^{-1}) = \sigma\varepsilon_0 E(z) \tag{4.26}$$

or

$$D(z) - z^{-1}D(z) = \sigma\varepsilon_0 E(z) \tag{4.27}$$

Performing inverse z-transform

$$D^n - D^{n-1} = \sigma\varepsilon_0 \Delta t E^n \tag{4.28}$$

Finally, for solving E from equation 4.28, we find

$$E^n = \frac{D^n - D^{n-1}}{\sigma\varepsilon_0\Delta t} \tag{4.29}$$

Which is same as the final update equation derived by ADE method.

4.3.3 Piecewise Linear Recursive Convolution Method

Luebbers et al. formulated the first frequency dispersive FDTD algorithm using the recursive convolution (RC) scheme. Later it became piecewise linear recursive convolution(PLRC) method [36]. Initially developed for Debye media [35], the approach was later extended for the study of wave propagation in a Drude material [37], N-th order dispersive media [38], an anisotropic magneto-active plasma [39], ferrite material [40] and the bi-isotropic/chiral media [41] [42] [43].

The RC approach, typically being faster and having required fewer computer mem-ory resources than other approaches, is usually less accurate. But in case of mul-tiple pole mediums, it is easier to follow the RC approach.

In the initial derivation of PLRC method for a linear dispersive medium, the re-lation between electric flux density and electric field intensity is expressed as:

$$D(t) = \varepsilon_\infty \varepsilon_0 E(t) + \varepsilon_0 \int_0^t E(t-\tau)\chi(\tau)d\tau \qquad (4.30)$$

which can be discretized as:

$$D^n = \varepsilon_\infty \varepsilon_0 E^n + \varepsilon_0 \int_0^{n\Delta t} E(n\Delta t - \tau)\chi(\tau)d\tau \qquad (4.31)$$

The PRC method is further preceded from this basing discrete equation.

4.3.4   The General Algorithm

The derivation of equations for multi-pole dispersion relation is more difficult compared to the single pole-pair dispersion relation. For example, for six-pole Lorentz-Drude dispersion the required derivation process is lengthy. Additionally, the memory required for computation is also vast. There are various methods proposed by researchers regarding this topic such as Taflove's matrix inversion method, Multi-term

dispersion by Okoniewski, etc. However Alsunaidi and Al-Jabr proposed a general algorithm technique which solves various problems regard-ing previous methods. The major advantage of this technique is that it requires only one algorithm for anyt dispersion relation. The dispersive relation has the general form as

$$D(\omega) = \varepsilon(\omega)E(\omega) \tag{4.32}$$

which can be expressed in terms of summation of poles

$$D(\omega) = \varepsilon_\infty \varepsilon_0 E(\omega) + \sum_i^N P_i(\omega) \tag{4.33}$$

where N is the number of poles. Applying Fourier transform, this equation becomes

$$D^{n+1} = \varepsilon_\infty \varepsilon_0 E^{n+1} + \sum_i^N P_i^{n+1} \tag{4.34}$$

or

$$E^{n+1} = \frac{D^{n+1} - \sum_i^N P_i^{n+1}}{\varepsilon_\infty \varepsilon_0} \tag{4.35}$$

This term P_i can be any form of dispersion relation such as the Debye, the Drude or just the conductivity term. This the final solved equation for E.

Chapter 5

Parameter Extraction of Optical Materials

The Modified Debye Model (MDM) parameters for silver metal is presented. A nonlinear optimization algorithm has been developed in order to extract the parameters for the metals. The extracted parameters have been used to determine the complex relative permittivity of the metals in optical and near-IR region of electromagnetic spectrum. The obtained results have been compared with the experimental values and an excellent agreement has been found.

5.1 Material Models

5.1.1 Modified Debye Model

5.1.1.1 Metals

The complex relative permittivity function of the modified Debye model is de-scribed by the following equation

$$\varepsilon_r(\omega) = \varepsilon_\infty + \frac{(\varepsilon_s - \varepsilon_\infty)}{1 + j\omega\tau} - j\frac{\sigma}{\omega\varepsilon_0} \tag{5.1}$$

where, ε_∞ is the infinite frequency relative permittivity, ε_s is the zero frequency relative permittivity, ω is the angular frequency, σ is the conductivity and τ is the relaxation time.

If the model is represented in terms of its real and imaginary parts, then,

$$\varepsilon_r(\omega) = \varepsilon'(\omega) - j\varepsilon''(\omega) \tag{5.2}$$

where, the real part of the complex relative permittivity is,

$$\varepsilon'(\omega) = \varepsilon_\infty + \frac{(\varepsilon_s - \varepsilon_\infty)}{1 + (\omega\tau)^2}$$

and the imaginary part of the complex relative permittivity is,

$$\varepsilon''(\omega) = \frac{(\varepsilon_s - \varepsilon_\infty)}{1 + (\omega\tau)^2} + \frac{\sigma}{\omega\varepsilon_0}$$

From equation 5.1, we can see that the modified Debye model can be described by four parameters which are ε_s, ε_∞, σ and τ. However, a relationship can be derived among these parameters by comparing equation 5.1 with the Drude model equation as,

$$\sigma = \frac{\varepsilon_0(\varepsilon_s - \varepsilon_\infty)}{\tau} \tag{5.3}$$

Now we actually have three parameters that need to be extracted and the other can be obtained from equation 5.3.

5.1.1.2 Dielectric Materials

The frequency dependent permittivity function of Modified Debye Model is given by

$$\varepsilon_r(\omega) = \varepsilon_\infty + \frac{(\varepsilon_s - \varepsilon_\infty)}{1 + j\omega\tau} \tag{5.4}$$

where, ε_∞ is the infinite frequency relative permittivity, ε_s is the zero frequency relative permittivity, ω is the angular frequency and τ is the relaxation time.

From equation 5.4 we can see that modified Debye model for dielectric material can be described by three parameters which are ε_∞, ε_s and τ. These three parameters need to be optimized in order to model dielectric materials using MDM.

5.1.2 Lorentz Model

The frequency dependent complex permittivity function for single pole-pair Lorentz model is given by

$$\varepsilon_r(\omega) = \varepsilon_\infty + \frac{\omega_0^2\,(\varepsilon_s - \varepsilon_\infty)}{\omega_0^2 + j2\delta\omega - \omega^2} \tag{5.5}$$

where, ε_∞ is the infinite frequency relative permittivity, ε_s is the zero frequency relative permittivity, ω_0 is the frequency of the pole pair and δ is the damping frequency.

From equation 5.5, it can be observed that single pole-pair Lorentz model can be described by four parameters which are ε_∞, ε_s, ω_0 and δ. These four parameters are independent and need to be extracted.

5.1.3   Developing the Simulation Model

The simulation model we have developed is based on the FDTD method. We have utilized the general auxiliary differential equation (ADE) based FDTD approach in order to incorporate the frequency dependent dispersion property of the constituent materials. This algorithm is useful for the simulation of materials with different dispersive properties. The perfectly matched layer has been integrated at all the boundaries in order to prevent back reflections.

Considering the material dispersion, the frequency-dependent electric flux density can be given by-

$$D(\omega) = \epsilon_o \epsilon_\infty E(\omega) + P(\omega). \tag{5.6}$$

The general Lorentz model for polarization (ω) is given by-

$$P(\omega) = \frac{a}{b + jc\omega - d\omega^2} E(\omega), \tag{5.7}$$

By inverse Fourier transform, it can be written in time domain as-

$$bP(t) + cP'(t) + dP''(t) = aE(t). \tag{5.8}$$

Now, turning to FDTD scheme, above equation can be presented as-

$$P^{n+1} = C_1 P^n + C_2 P^{n-1} + C_3 E^n. \tag{5.9}$$

Where, $C_1 = \dfrac{4d - 2b\Delta t^2}{2d + c\Delta t}$, $C_2 = \dfrac{-2d - c\Delta t}{2d + c\Delta t}$, and $C_3 = \dfrac{2a\Delta t^2}{2d + c\Delta t}$.

The values of C_1, C_2, C_3 depends on the material under consideration. Finally, equation of field intensity has the form-

$$E^{n+1} = \frac{D^{n+1} - \sum_{i=1}^{N} P_i^{n+1}}{\epsilon_0 \epsilon_\infty} \tag{5.10}$$

Where N is the number of poles and D^{n+1} is the next value of electric flux density after one iteration in FDTD algorithm.

Chapter 6

Designing Plasmonic Diode

6.1 Introduction

The propagation of Surface Plasmon Polariton can be used for the simulation of plasmonic diode. Having developed the simulation model, structures can be such a way that the plasmon propagation takes place in certain direction and doesn't in the opposite. This idea can be used to implement the plasmonic diode. Suitable materials are to be chosen for the closest implementation of the idea. However, it's not possible to make the plasmonic diode like the ideal one, but can be modeled for very good performance by varying different parameters which would be discussed in the later sections.

6.2 Plasmonic Diode Strucures

6.2.1 Basic Diode Structure

In the structure designed here, there are two air films sandwiched within Silver (Ag). The films are placed perpendicular to each other within the silver substrate. The perpendicular positioning of the structure will naturally allow the plasmon propagation to a certain direction and eventually block in the other direction. However, the frequency of the used signal would greatly affect the propagation of the plasmon profile.

The structure is composed of Silver substrate of dimension 1000nm x 1000nm. The two air films are seen in the figure. The designed width of the Air films is 100nm. The horizontal one of the two Air films is 100nm above from the bottom. The vertical Air film is 500nm right from the leftmost plane of the Silver substrate. Height of the vertical film is 900 nm.
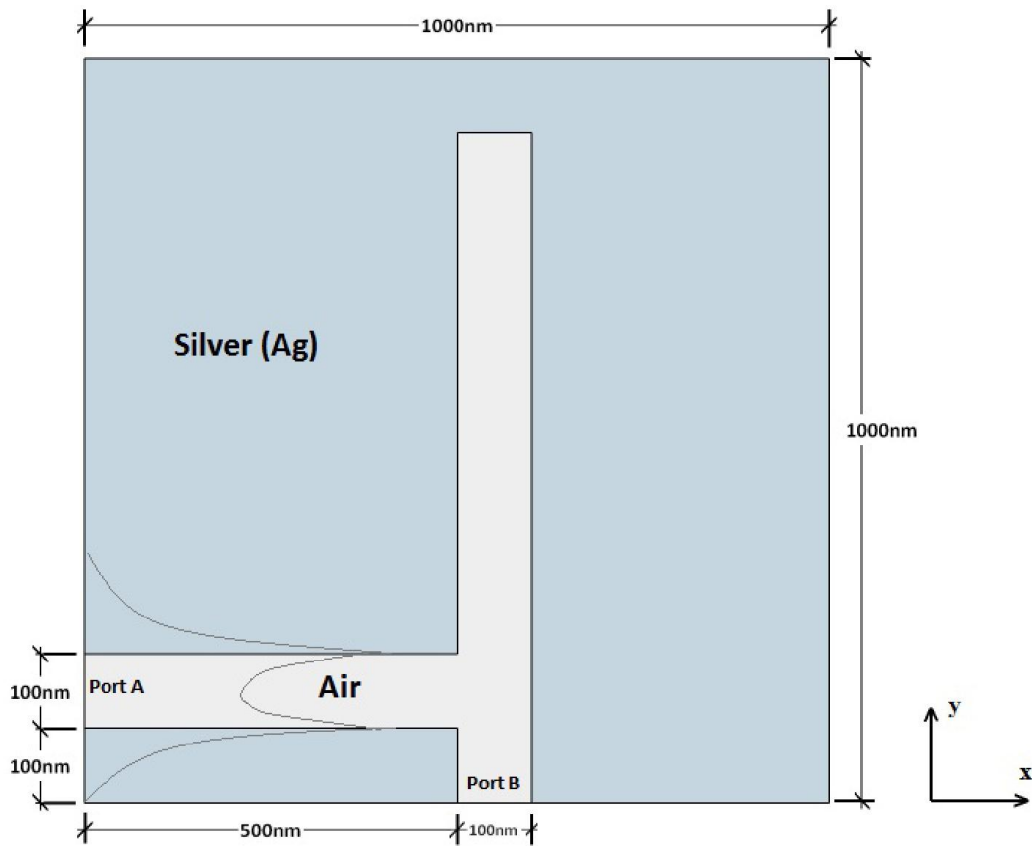
Fig 6.1: Basic Plasmonic diode structure.

Now, ports have been assigned for making analogy with ordinary diodes. As seen from the figure, leftmost point on the horizontal Air film is the Port A whereas point at the most bottom of the vertical Air film is assigned as Port B. Now, since we've developed the general simulation model for any structure, we can simulate how a plasmonic profile would propagate through the structure for incidences at the different ports.

6.2.2 Simulation of the Plasmon Profile Propagation through the Diode

For the simulation of the plasmon profile propagation, firstly plasmon profile is generated by the incidence of a photon pulse on the interface. Below are the E_x, E_y, Hz fields for the generated plasmon profile-

normalized Ex field

normalized Ey field
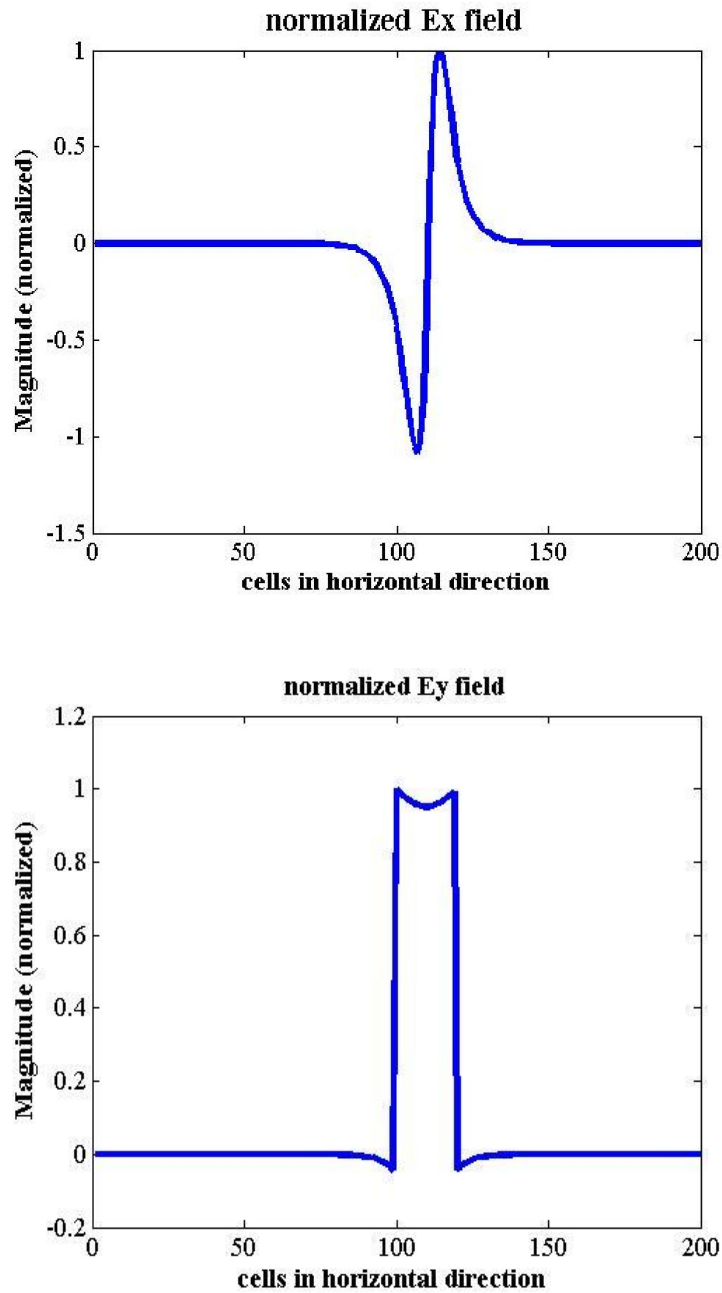
Fig 6.2: Ex,Ey profiles for the generated plasmon
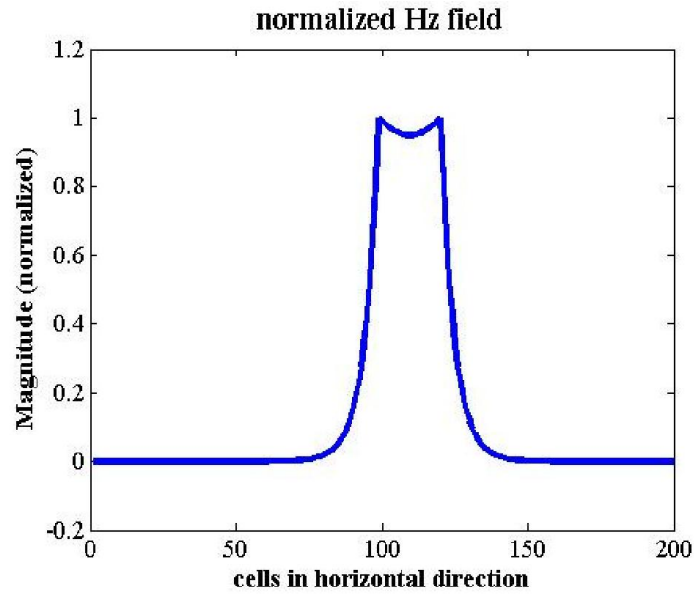
Fig 6.3: H_z profiles for the generated plasmon

These profiles will be sent through both the ports one by one. Firstly we choose port A where the generated Plasmon profile is incident. Using FDTD method and those obtained models, we can generate the propagation profiles at different times. The profile propagates well in the dielectric medium, here Air. But it doesn't propagate through the metal since it's a lossy medium. The simulation figures are presented in the following. First four figures are the simulation profiles at different time steps taken gradually for the incidence in port A, whereas the next four figures are for the incidences at port B.
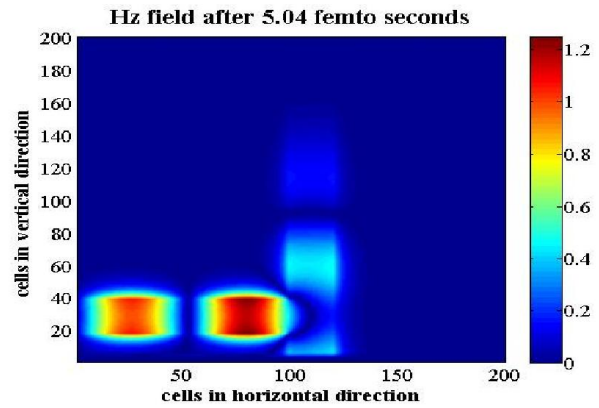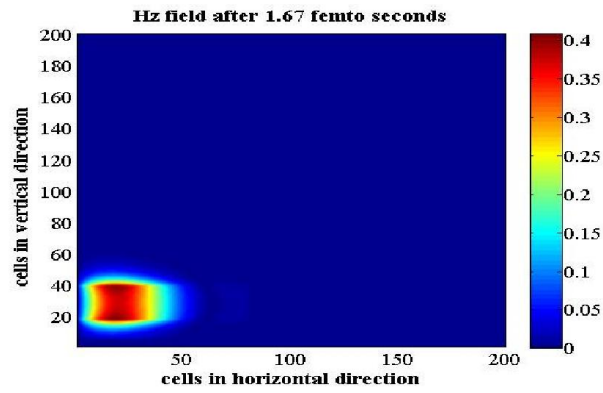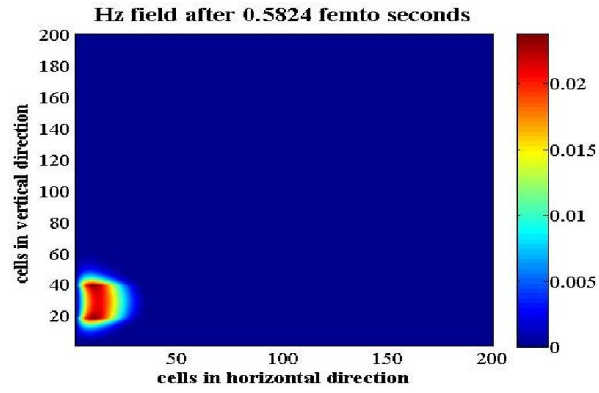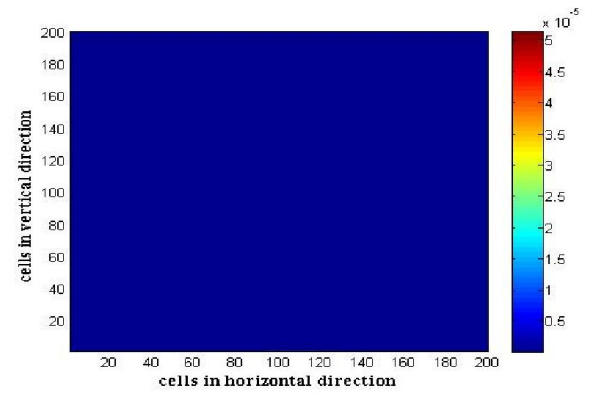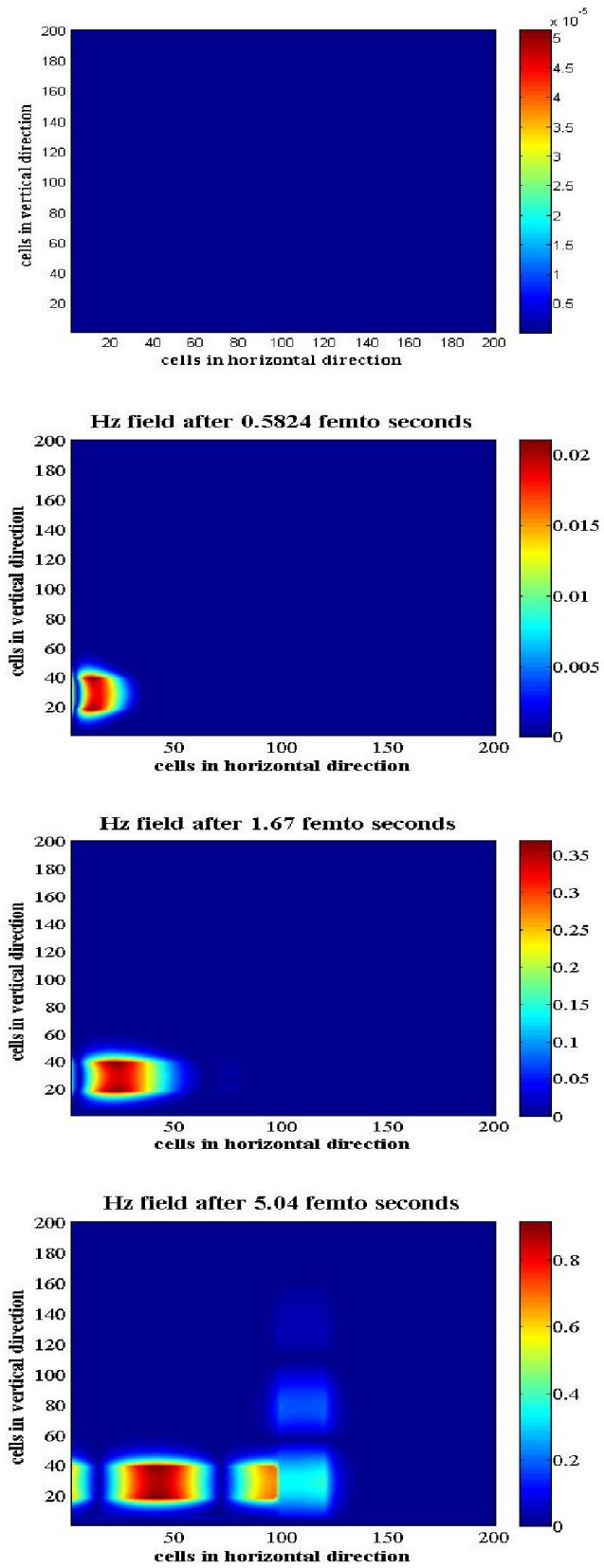
Fig 6.4 snapshot of Hz field when input is in port A
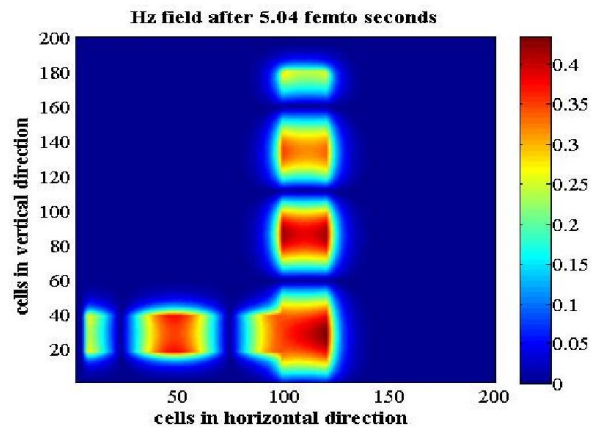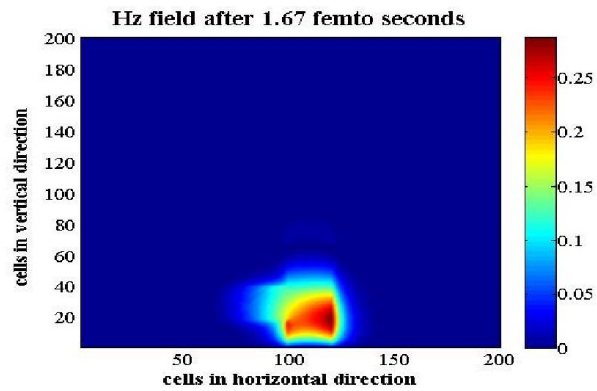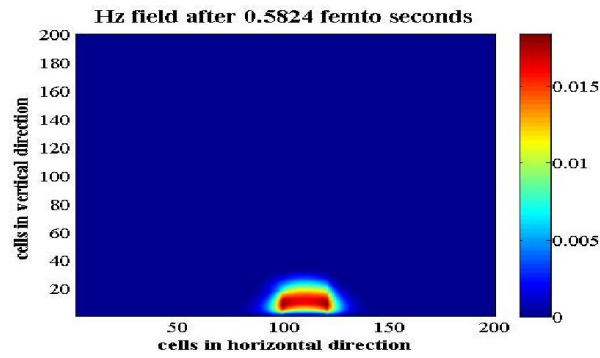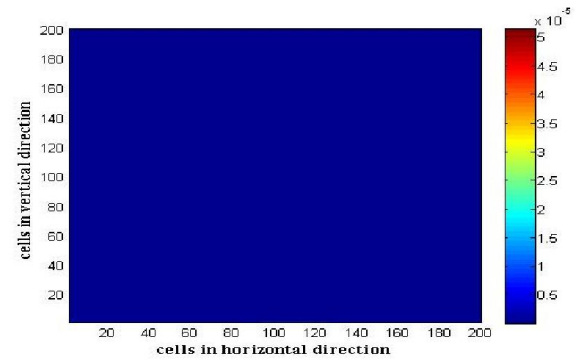
Fig 6.5 snapshot of Hz field when input is in port B

6.3 Modification of the Proposed Structure

6.3.1 First Modification

A gap of 10nm have been inserted in between the horizontal and vertical Air films. So, the horizontal Air film now stretches up-to 490 nm. The other dimensions are kept the same. It can be visualized properly from the figure.
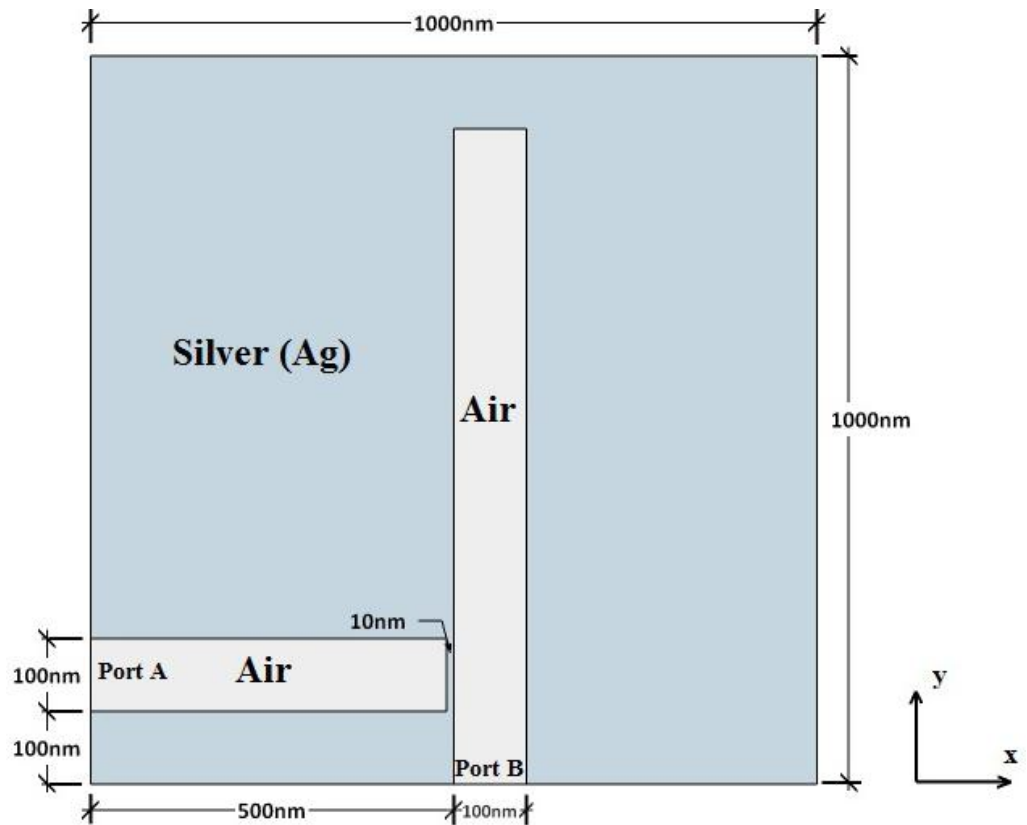
Fig 6.6: Insertion of 10 nm gap in between the air films.

We can now go through similar simulations as the previous one to visualize the plasmon propagation in this modified structure. The inserted gap will have reasonable effect on the propagation of plasmon profile. The simulation profiles are presented in the following figures.

Fig 6.7 snapshot of Hz field when input is in port A
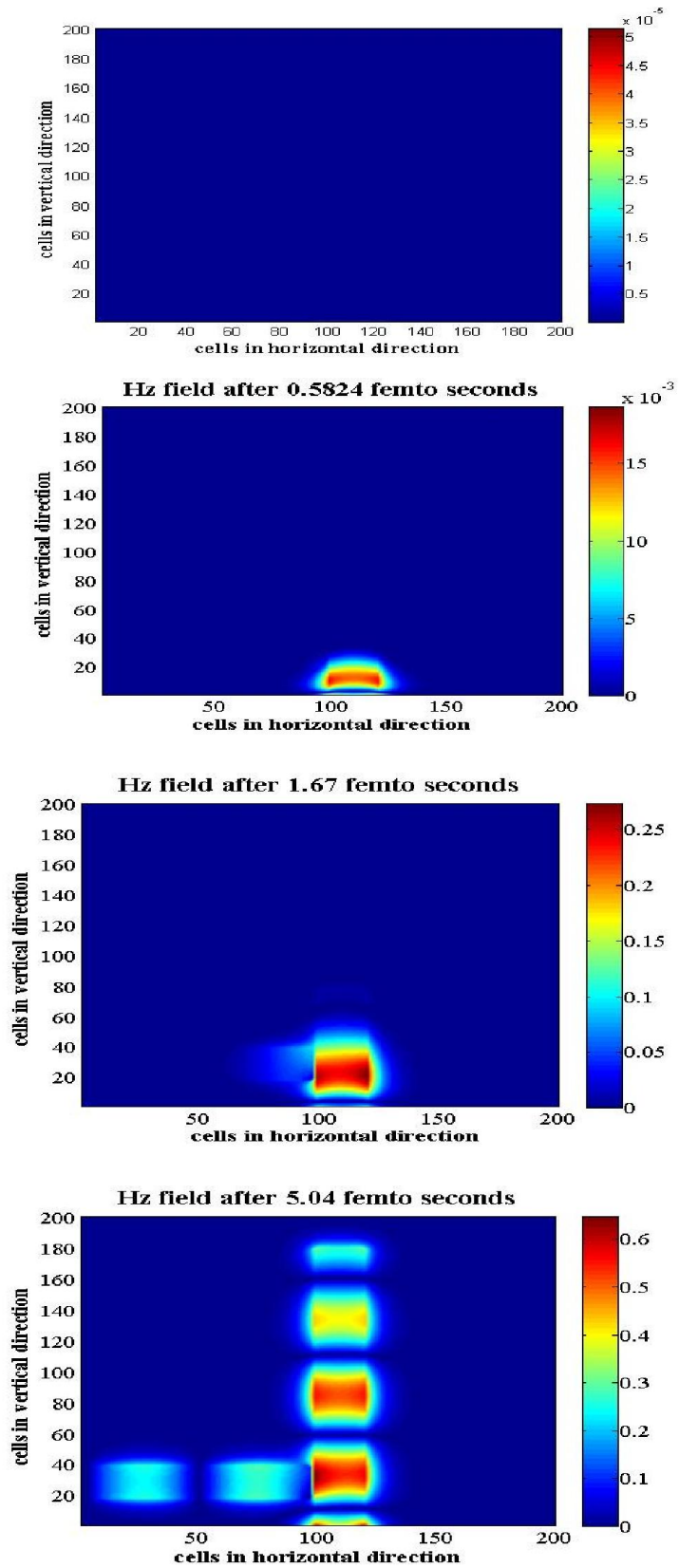
Fig 6.8 snapshot of Hz field when input is in port B

6.3.2 Second Modification

In the second modification of the structure, the metal gap in between the horizontal and vertical Air films has been increased to 20 nm. The length of the horizontal film now becomes 480 nm.
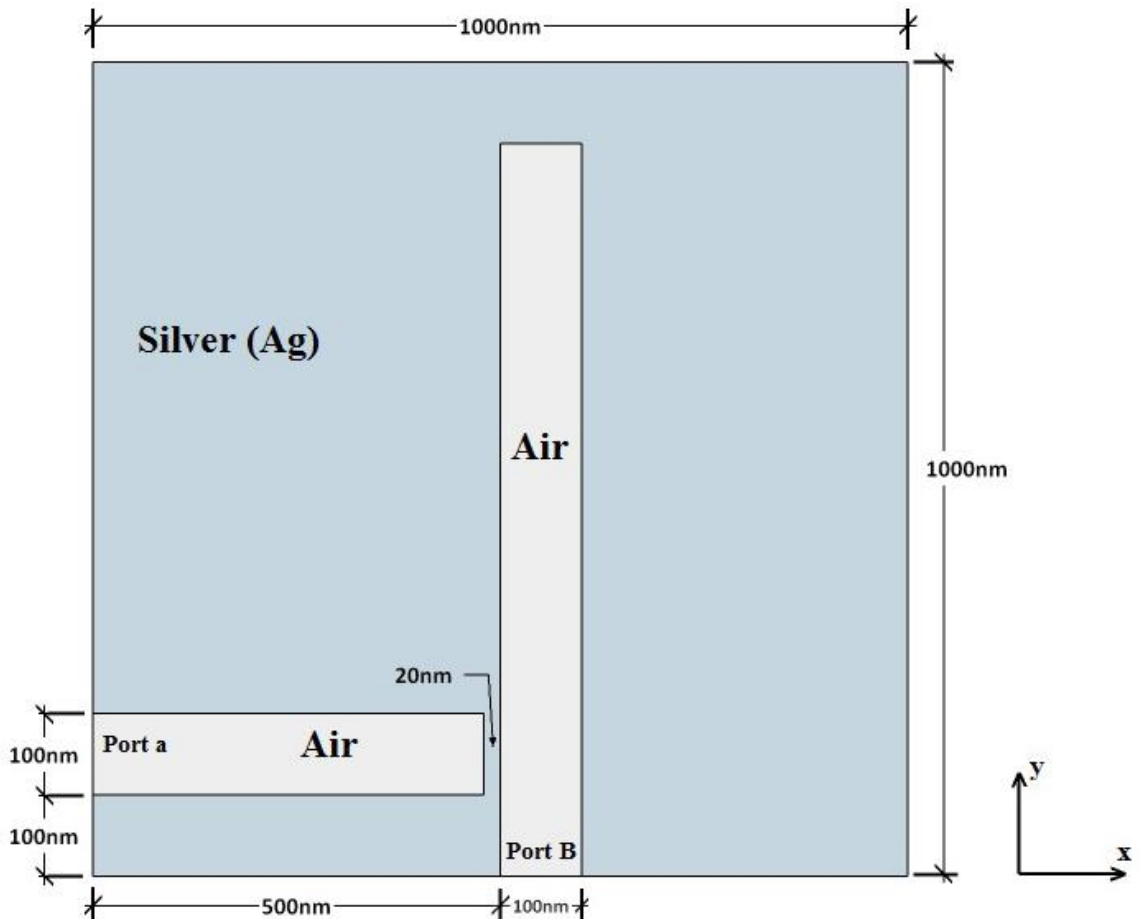
Fig 6.9: The metal gap increased to 20 nm.

Due to insertion and increase of the metal gap in first and second modifications, a lossy medium actually occurs in between the air films. This will definitely increase the loss of power inside the structure but it will increase the transmittance contrast to a great extent. The performance comparison would be shown in the following chapters. Here, the simulation figures for this second modification are presented.
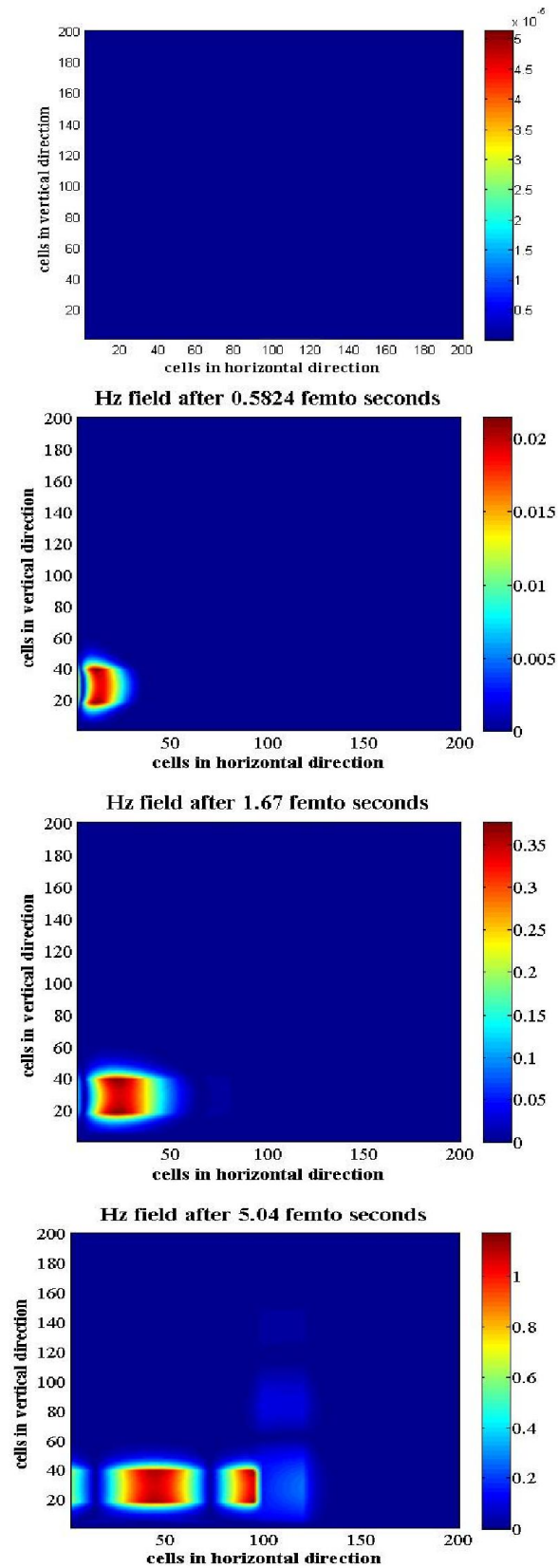
Fig 6.10 snapshot of Hz field when input is in port A
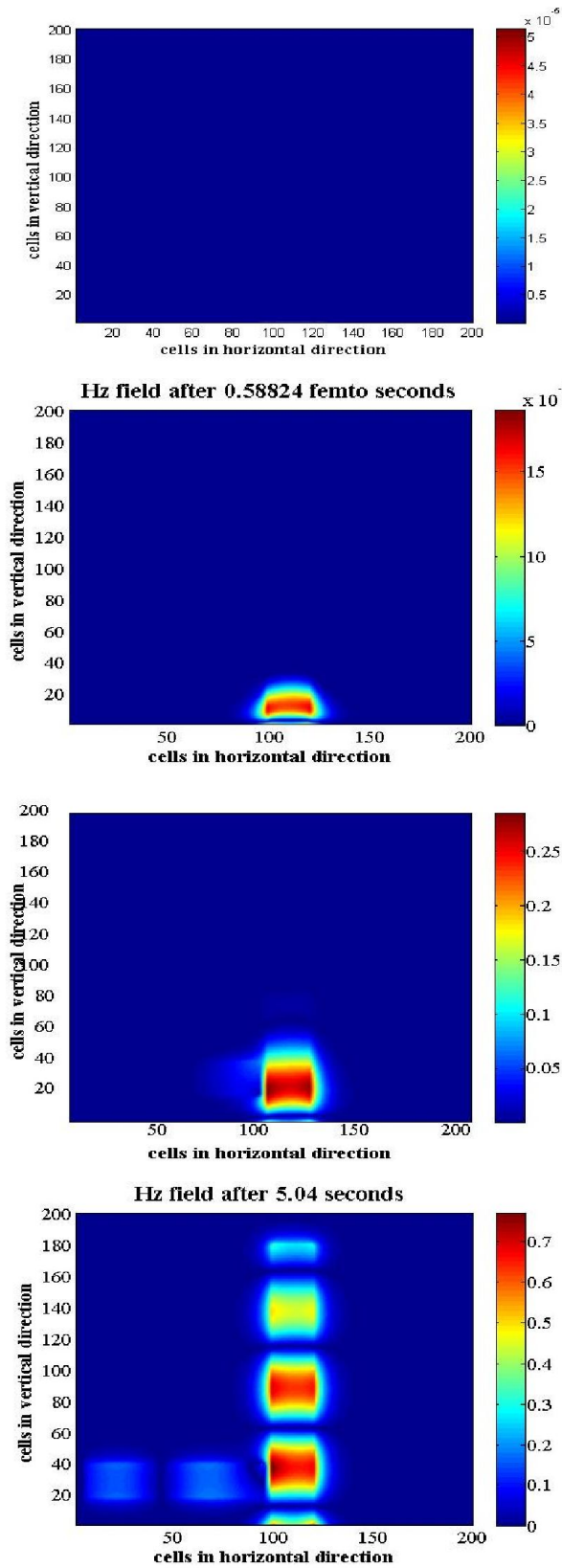
Fig 6.11 snapshot of Hz field when input is in port B

Chapter 7

Performance Analysis of Plasmonic Diode

7.1. Performance Analysis

7.1.1 Overview

For Plasmonic diodes, performance may be referred to how good it's working in forward and reverse biases. Generally. Transmittance contrast is the appropriate measure of the performance of the plasmonic diodes. However, in here, the energy passed through the diode is measured at both the ports one after another while the signal is incident on the other. The calculations have been done for varying wavelengths of the incident signal. Thus, from the plot of energy measured at the two ports vs. the wavelength of the incident signal, we can visualize the performance of the diode at different wavelengths. The appropriate wavelength for biasing the diode can also be found from the mentioned graphs.

7.1.2 Calculation of the Energy Passed through the Ports

For the purpose of calculating the energy, firstly the power at the ports for different time steps are calculated. To calculate the power at different time steps, Pyonting vector was

used. Pyonting vector is defined as the cross product of Electric and Magnetic field intensities at a certain instant or here, time step. Mathematically-

$$\vec{S} = \vec{E} \text{ x } \vec{H} \tag{7.1}$$

Where,

$\vec{S}$ = instantaneous power,

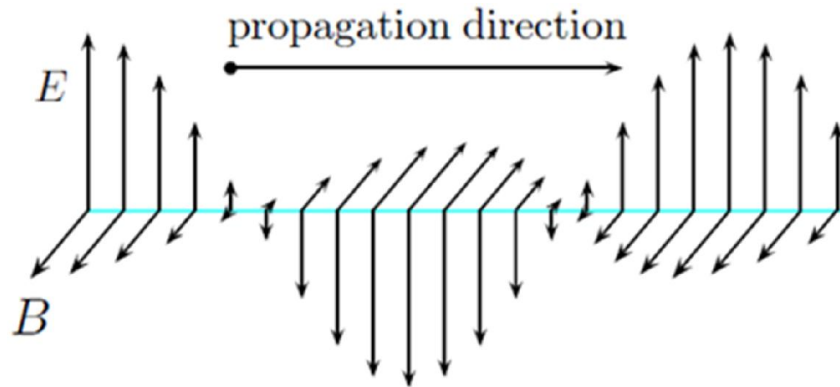$\vec{E}$ = Electric field intensities

$\vec{H}$ = Magnetic field intensities

Fig 7.1: E and H fields for calculating instantaneous power.

The power over the range of calculated time steps is found out by multiplying with the time step, we can find out the total energy passed through a particular port for a given no. of time steps. Mathematically, energy passed through will be given by-

$$Energy = |\vec{S}| * \Delta t \tag{7.2}$$

Where, Δt is the time step.

7.2 Performance of the Designed Diode

7.2.1 The Energy vs. Wavelength Curve

From the calculation methods described earlier, the obtained energy vs. the wavelength curve for the basic design is as Fig.
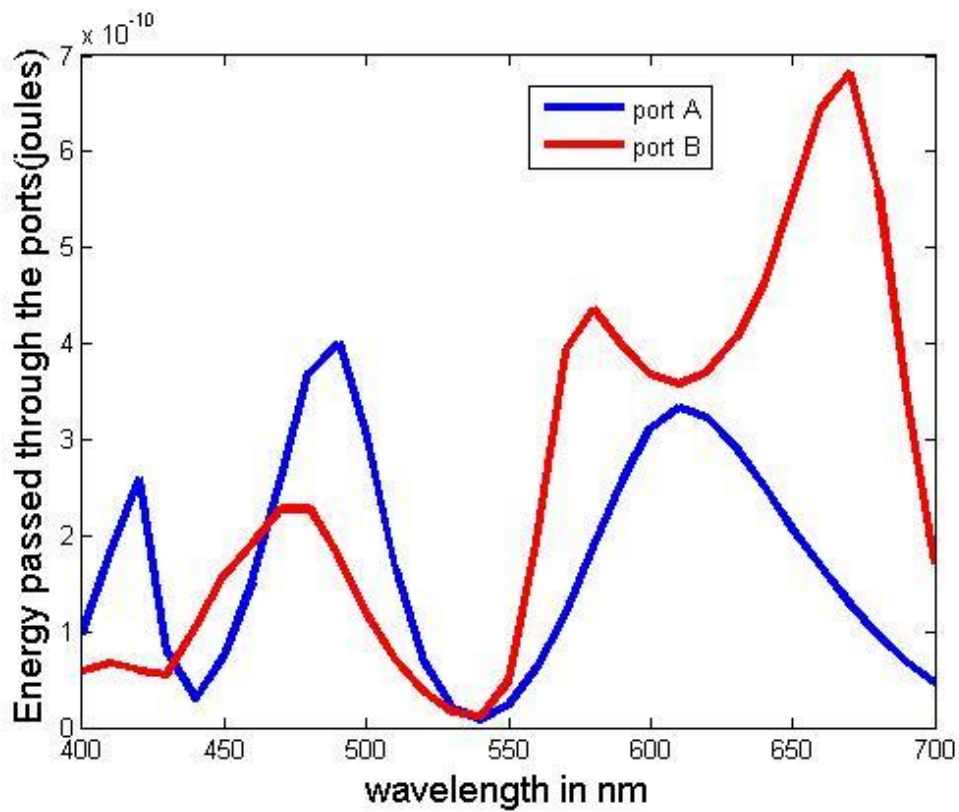

Fig 7.2: Energy passed vs. wavelength curve.

7.2.2 Analysis of the curve

As mentioned in the figure, Blue and Red lines represent energy passed through port A and port B whereas it's obvious that, the signal was incident in the other port. Here, the functionality of the ports varies randomly with wavelength. Though there are some distinct regions where the ports behave like a particular terminal like anode or cathode, it's not predictable and well defined. And also, during the implementation in any plasmonic circuits, the slight change in the used frequency may simply change the biasing of the diode. This is the reason the structure was modified.

7.3 Performance Analysis of the First Modified Structure

The first modification was the one with 10 nm metal gap in between the vertical and horizontal air films. So, the improvement on the biasing dependence on wavelength was observed.

7.3.1 Energy vs. Wavelength Curve
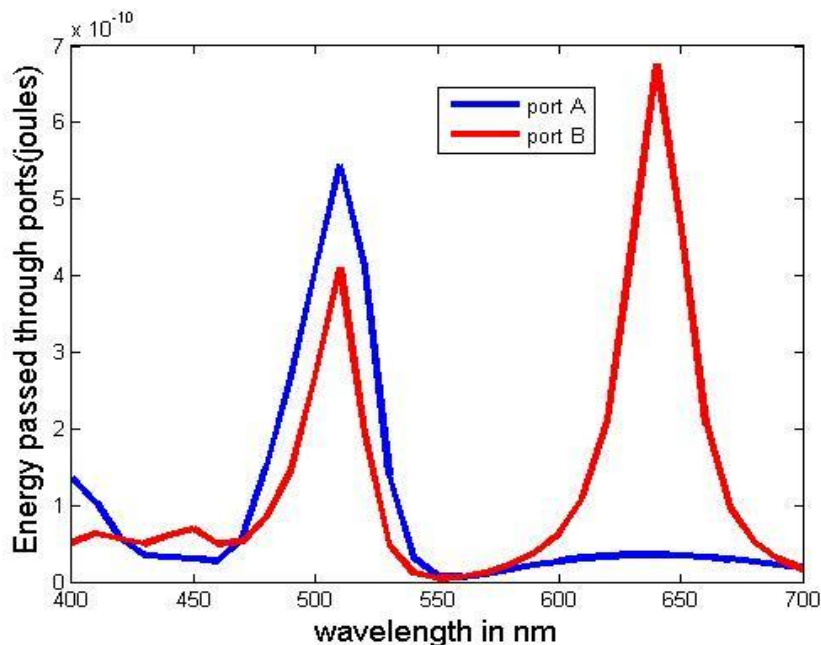
Fig 7.3: Energy passed vs. wavelength curve of modification 1

7.3.2 Analysis of the Curve

Here, we observe two particular wavelengths where the diode is seen to be forward biased and reverse biased. At around 640 nm, the best performance was observed. Here, port A act as anode and port B as cathode. Also, it's seen that opposite biasing occurs at around 510 nm. So, we can comment that the biasing has improved and also the frequency dependence property is mentionable.

7.4 Performance Analysis of Second Modified Strucuture

7.4.1 Transmitted Energy vs. Wavelength curve
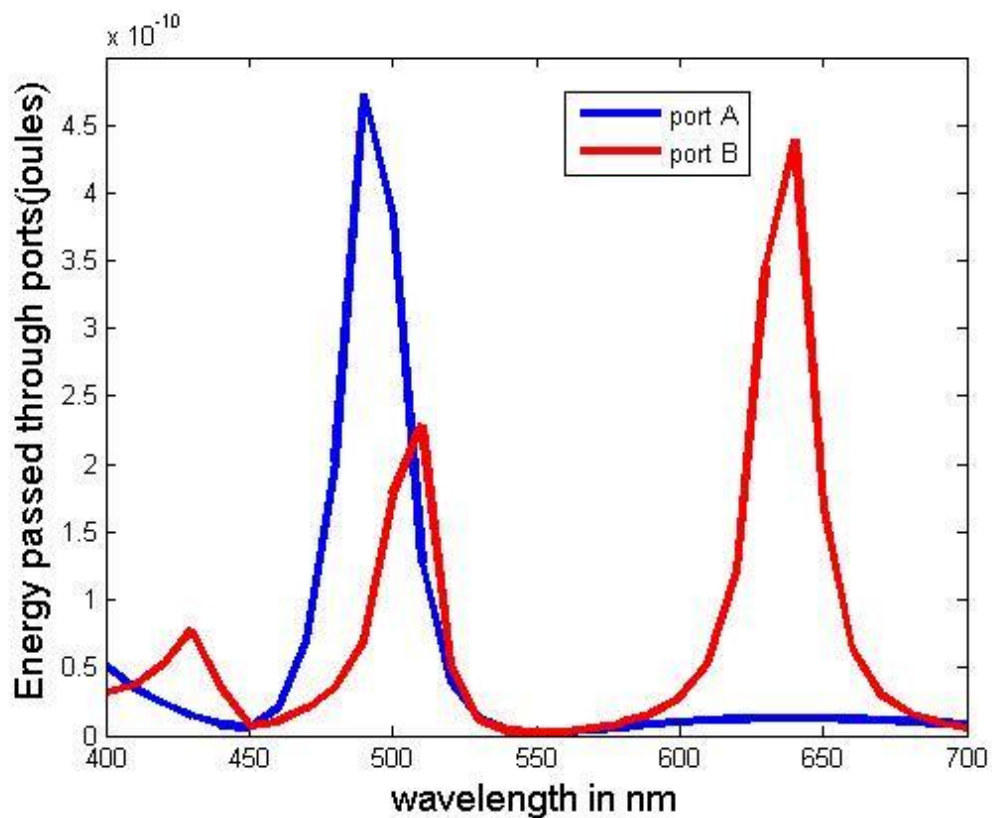
Fig 7.4: Energy passed vs. wavelength curve of modification 2

7.4.2 Analysis of the Curve

Here, the performance has improved further. At around 640 nm, we have port A as anode and port B as cathode. At 480nm, reverse situation occurs, and also the difference of energy passed increases at a great extent.

Chapter 8

Frequency Converter

8.1 Introduction

8.1.1 Background

As we have seen in previous chapter, the biasing properties of the designed diode varies with the frequency (or wavelength) of the used signal. So, to implement the designed diode effectively in a chip, the frequency of the signal is to be made suitable for the appropriate biasing of the diode. Consequently, necessity of a device to change the frequency of the signal suitably emerges. For this purpose, a frequency converter has been designed. This will be used in the same chip immediately after the diode to determine the biasing.

8.1.2 Working Mechanism

The property of polarization in different materials due to propagation of Electromagnetic waves through them has been exploited to implement the frequency converter. The electromagnetic waves while propagating through the materials, squeezes or expands according to the property of the material. In the input and output ports of the device, different materials have been used. As a result, the wave would go through expansion or

compression at the input or output due to different materials. Eventually we get our required signal. The frequency conversion will largely depend on material used and also the dimension of the films.

8.2 Designed Structure of the Frequency Converter

The dimension of the structure is 1000nm x 1000nm. Here a film of 100nm is sandwiched within Silver (Ag). The film stretches from 500nm to 600nm from the left side of the structure. The film composed of 500nm Air and 500nm AlAs as shown in the figure.
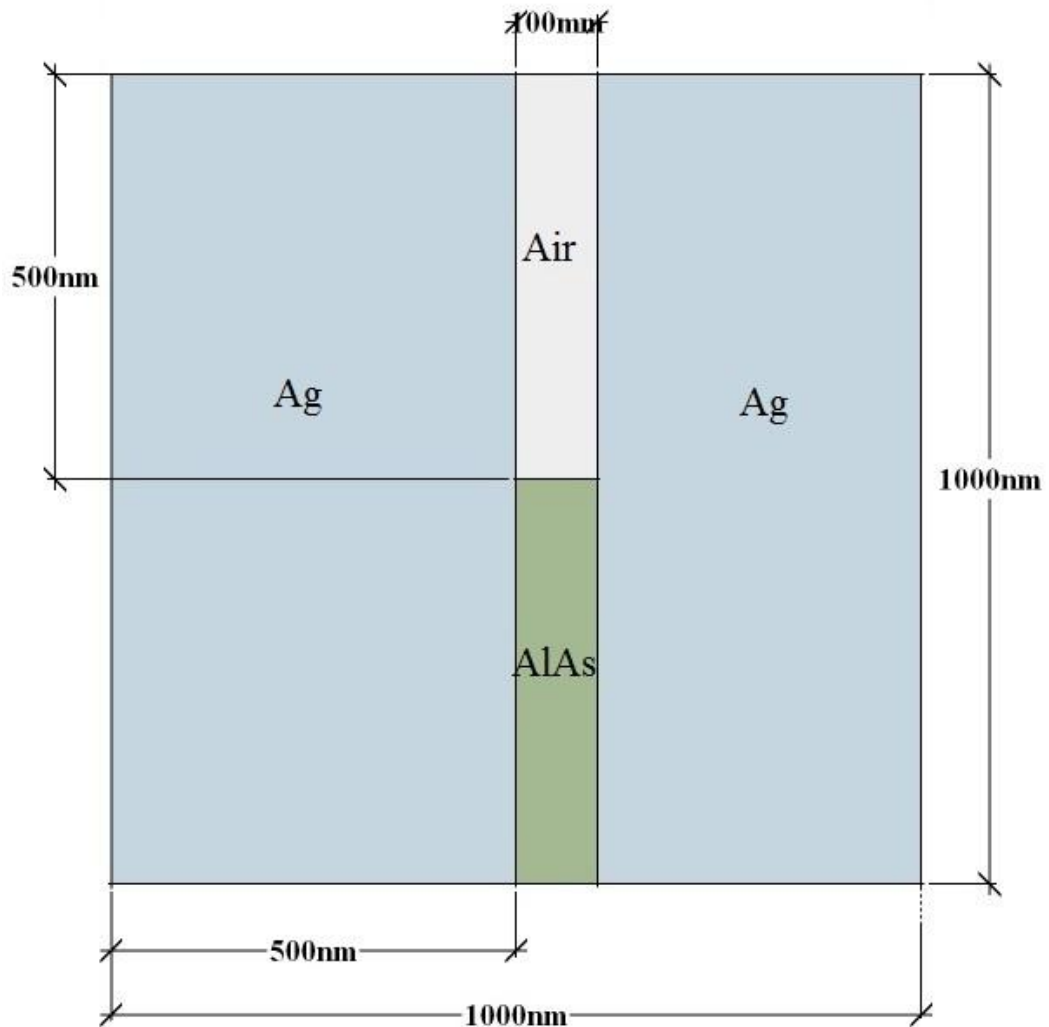

Fig 8.1: Structure of the designed frequency converter with AlAs-Air film

A similar design is also made replacing AlAs with GaLnS
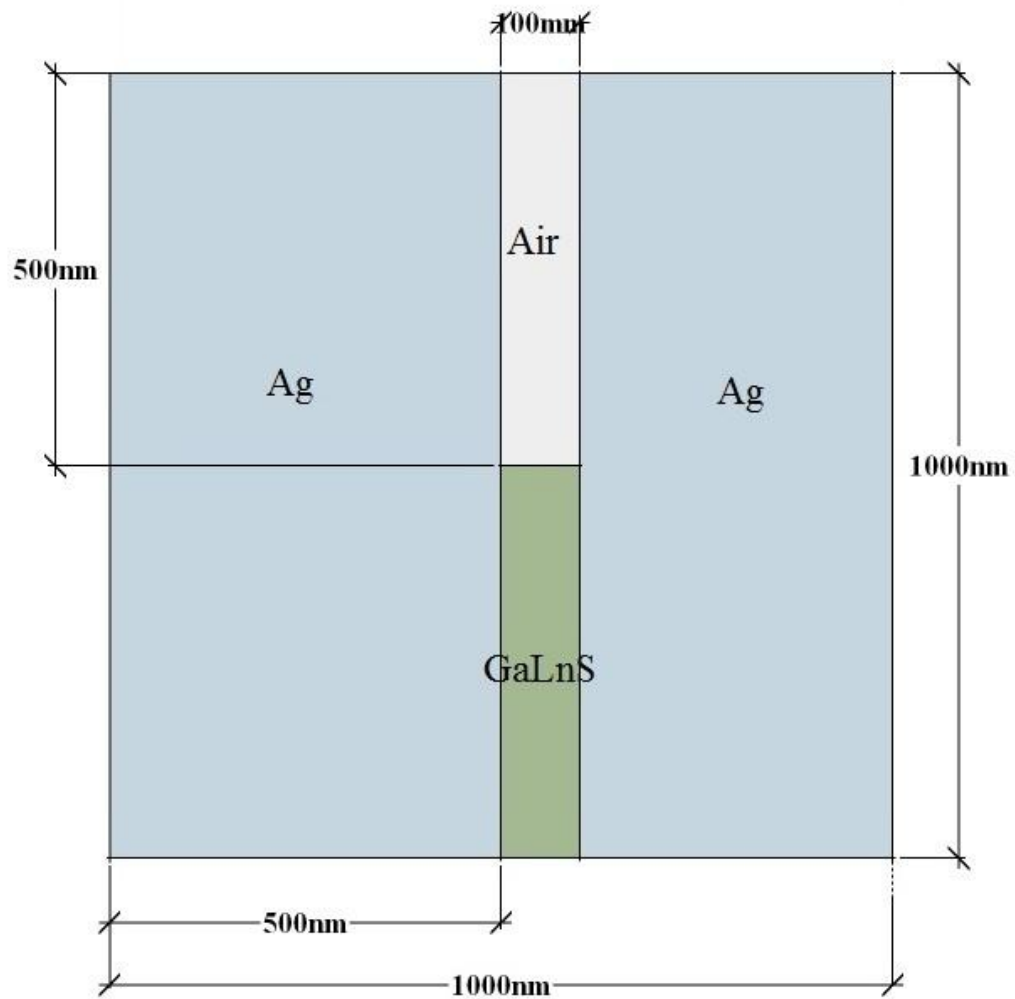
Fig 8.2: Structure of the designed frequency converter with GaLnS-Air film

8.3 Simulation of Propagation of EM Waves

The generated EM wave was incident at the two end of the film one by one. The intensity of the waves while passing through the film was obtained. Few of them at four different time steps are presented here. Firstly, the wave was incident from top i.e. Air. Later figures are for the incident at the AlAS or GaLnS side of the film.
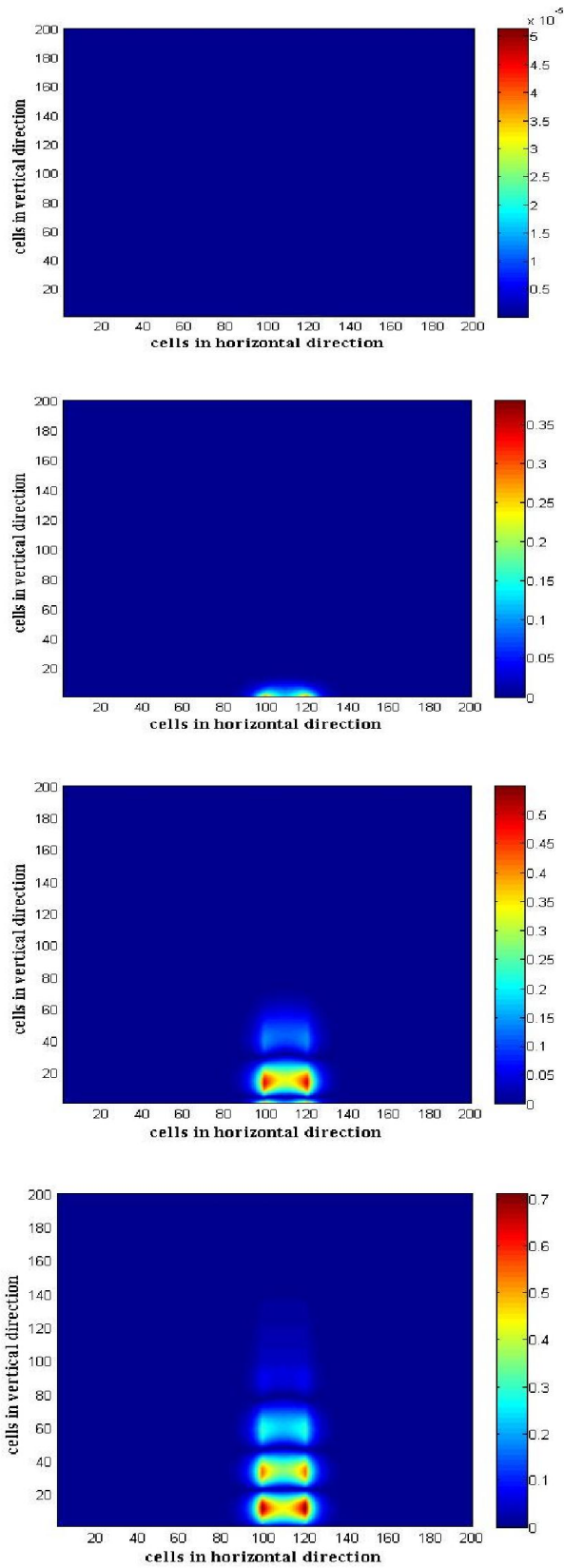
Fig 8.3: snapshot of Hz field distribution when the input is in GaLnS side
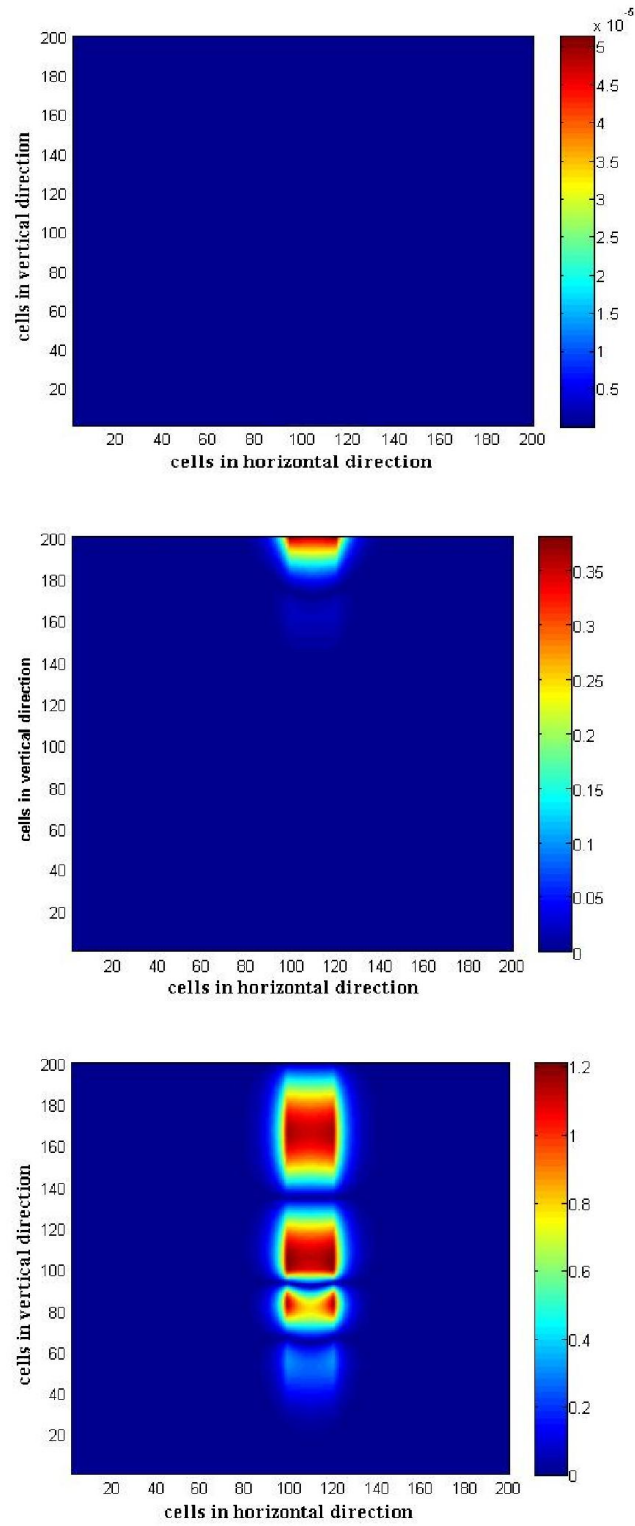
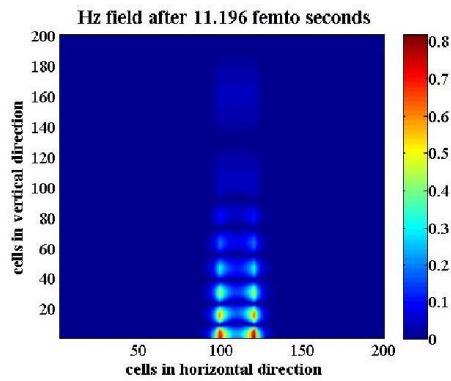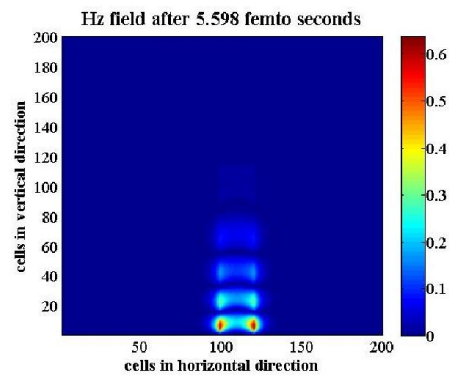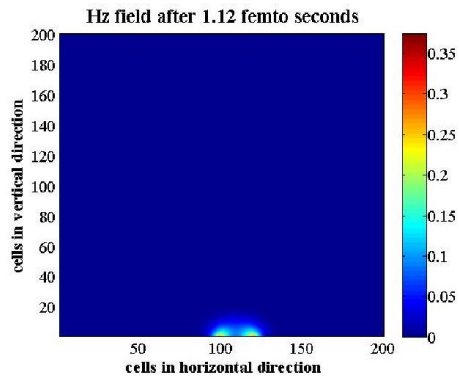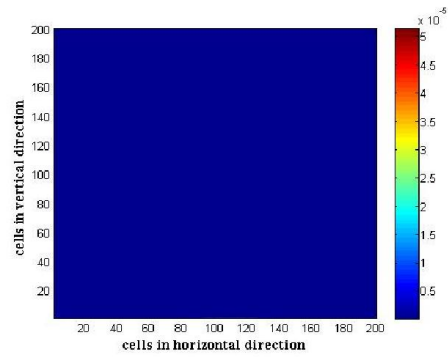Fig 8.4: snapshot of Hz field distribution when the input is in air side

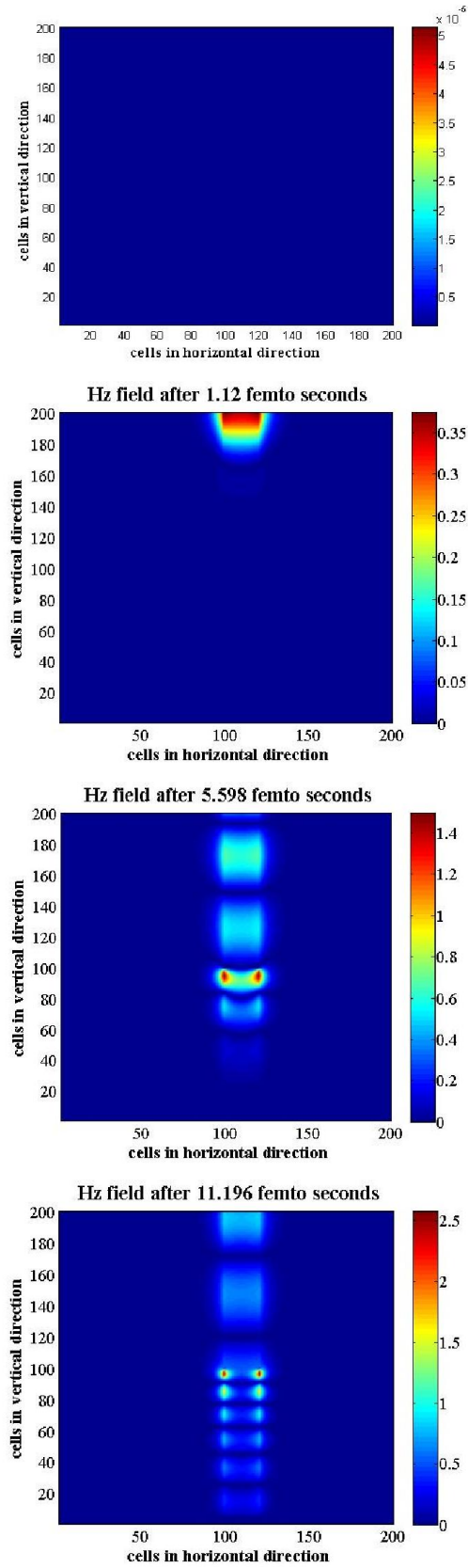Fig 8.5: snapshot of Hz field distribution when the input is in AlAs side

Fig 8.6: snapshot of Hz field distribution when the input is in air side

Chapter 9

Performance Analysis of Frequency Converter

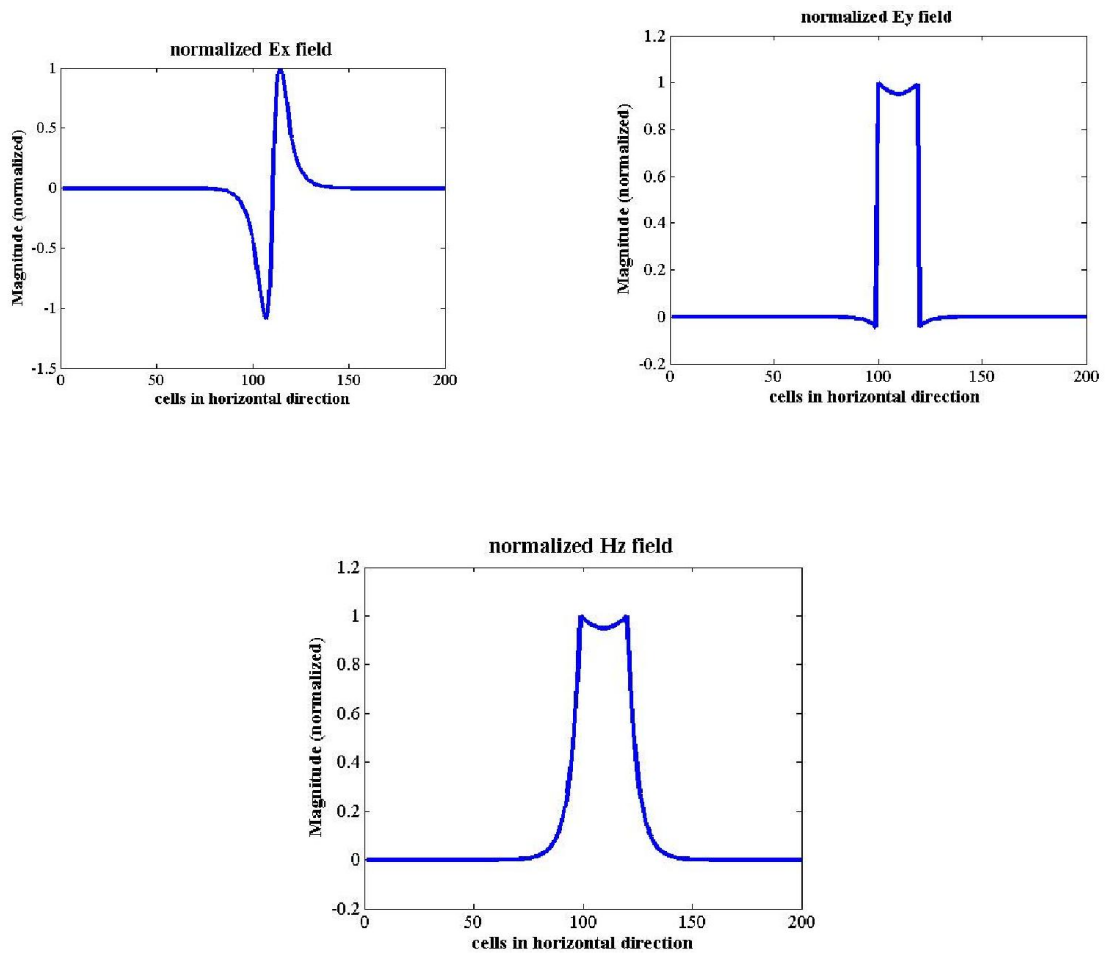## 9.1 Generated Profiles of Metal-Dielectric-Metal Interfaces
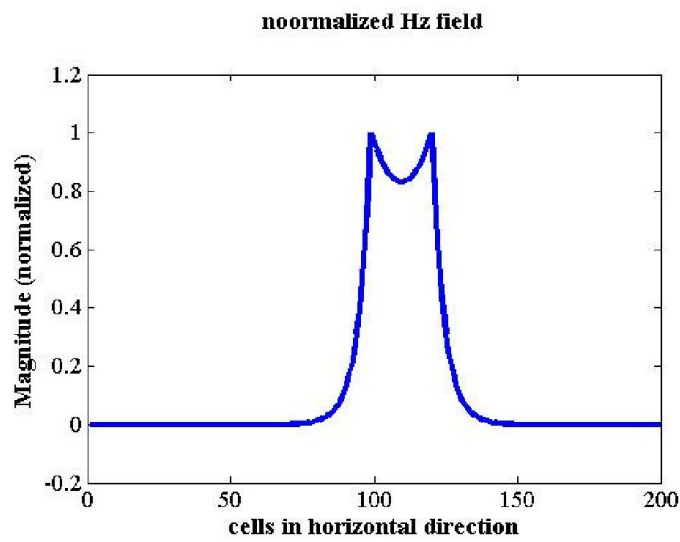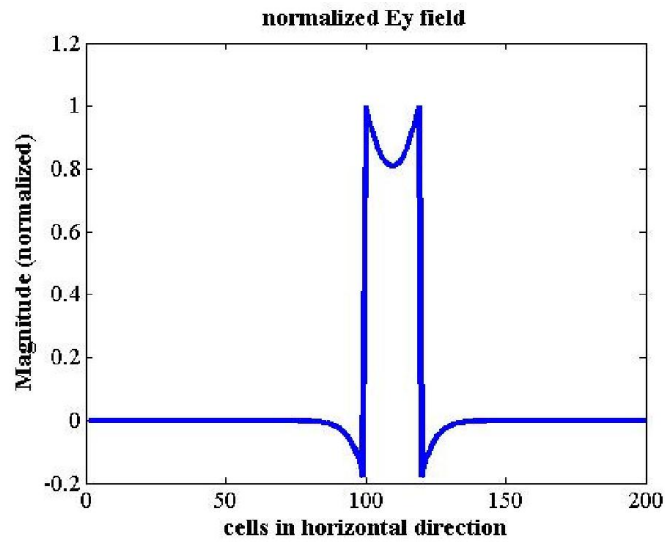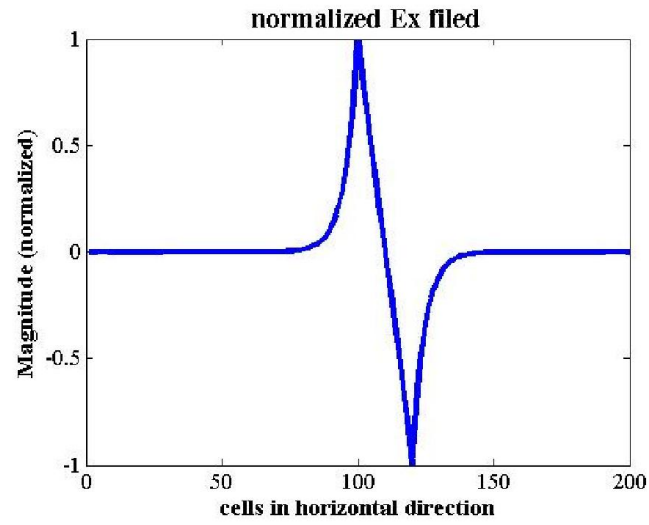

Fig 9.1: Normalized Ex,Ey,Hz field Ag-air-Ag interface

Fig 9.2: Normalized Ex,Ey,Hz field Ag-GaLnS-Ag interface
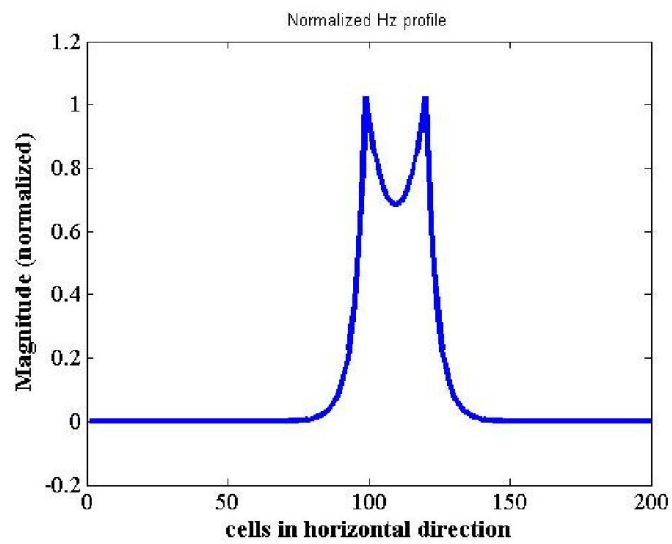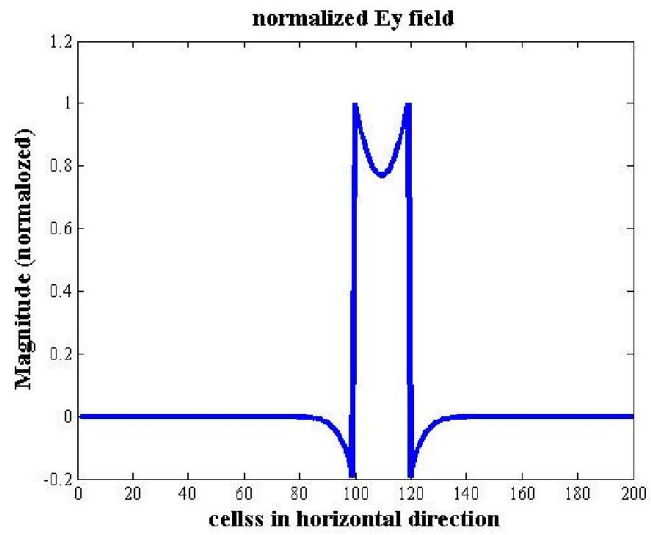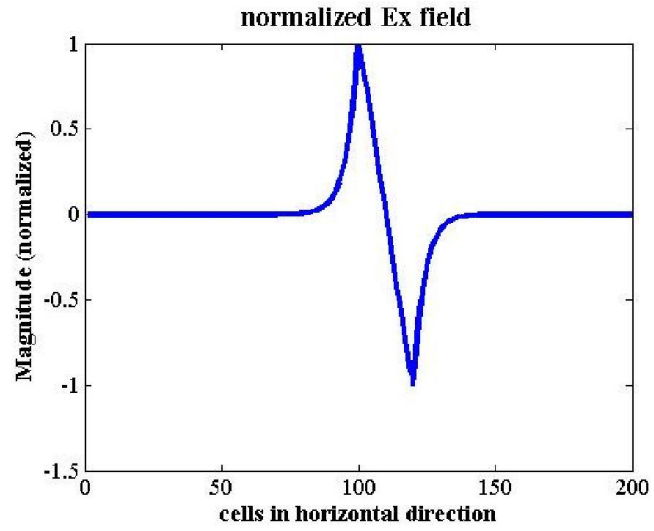
Fig 9.3: Normalized Ex,Ey,Hz field Ag-ALAs-Ag interface

9.2 Sectional View of the Waveguide

9.2.1 Wave Propagation through Air-AlAs Composite

Firstly, the wave is incident at the Air. Here it propagates up-to Air-AlAs junction with little loss. But when it enters the AlAs medium, the frequency of the signal increases as the wave is squeezed due to polarization. The loss is also higher which can be visualized from fig.9.4
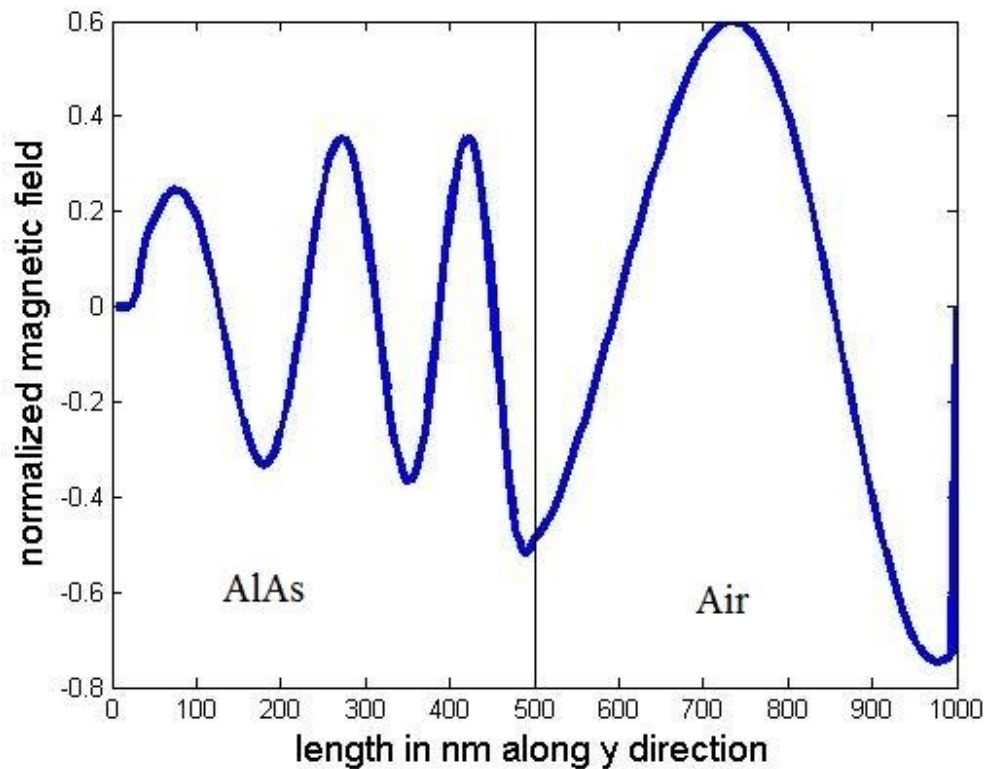
Fig 9.4: sectional view through AlAs-Air composite when the wave incidence at air side

Now, the wave is incident at AlAs side. Here also, the loss is prominently seen from fig. 9.5
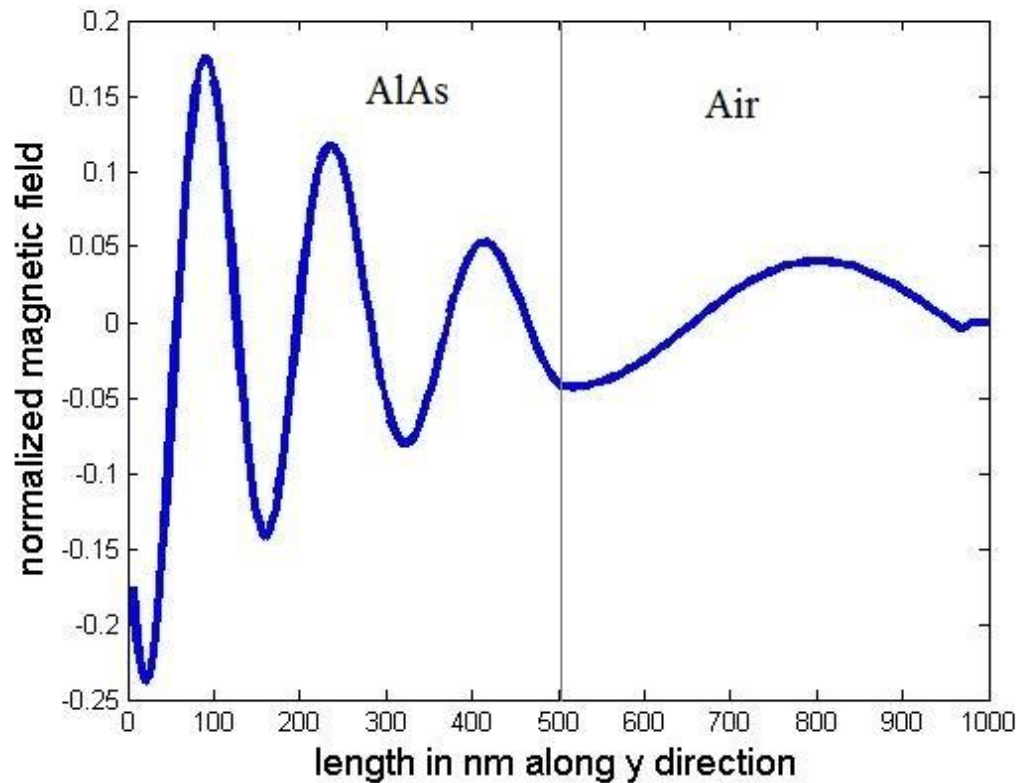
Fig 9.5: sectional view through AlAs-Air composite when the wave incidence at AlAs side

9.2.2 Wave Propagation through Air-GaLnS Composite

The similar simulation is done with Air-GaLnS Composite. Firstly, we observe the propagation for incidence at Air. Here, the propagation after the junction inside GaLnS is the matter of interest. The loss in GaLnS medium is much less than in AlAs.
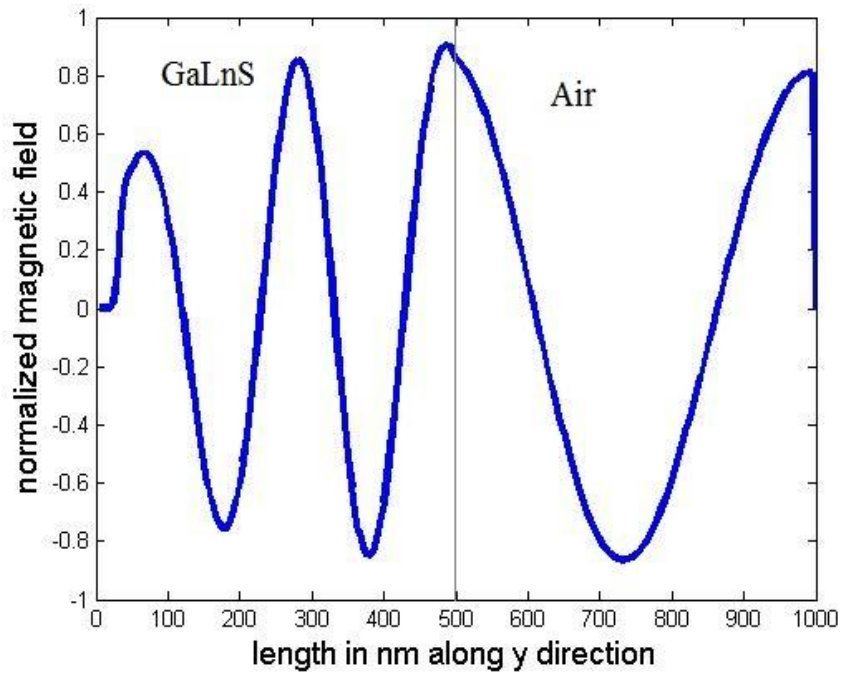
Fig 9.6: sectional view through GaLnS-Air composite when the wave incidence at air side

Similar simulation is done with the wave incident at GaLnS medium. As expected, the loss is much less. However, there's significant loss at the Air-GaLnS junction.
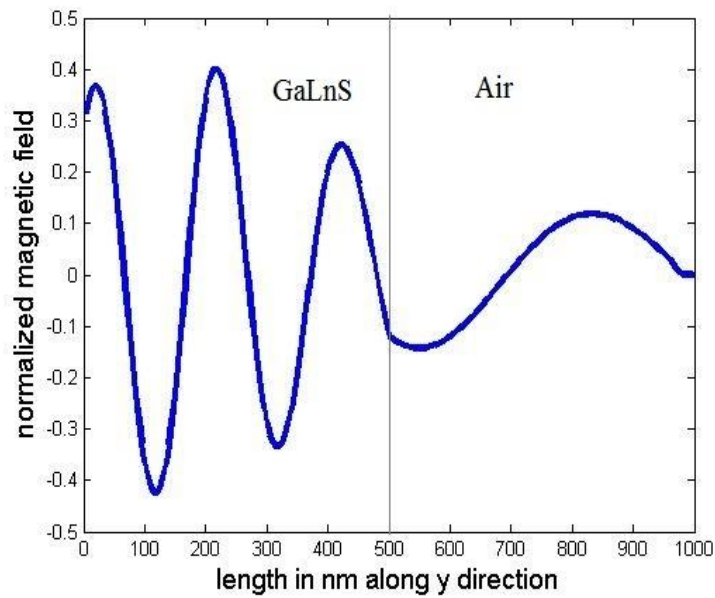
Fig 9.7: sectional view through AlAs-Air composite when the wave incidence at GaLnS side

Chapter 10

Conclusion and Future work

10.1 Conclusion

Here, thorough analysis of the designed devices were done. The transmitted energy at different ports at different frequencies gave the idea about the functionality of the ports. The sectional view of the frequency converter gave better idea of its performance. The accomplished tasks can be summarized as follows-

- The plasmonic diode was designed and the functionality of the ports was validated for different frequencies.
- To have better frequency dependency of the diode biasing, two modifications were also proposed. It enables us further improvement of the device by changing the design parameters.
- A frequency converter was designed to provide proper biasing to the designed diode
- The working mechanism of the frequency converter was clarified by proper illustrations like sectional views.

10.2 Future Works

In future, we have the plan to work on other devices and also improve the designed ones by further analyses. To give more particular view of the planned future works, following list is provided-

- To find more appropriate analysis of performance of the plasmonic diode by calculating transmission contrasts.
- To represent the performance of the frequency converter by spectrum and also find the conversion dependency on composite film dimensions
- To design other plasmonic devices like NAND ,NOR, NOT etc. logic gates
- To design a simulator that can simulate 2-D simulation of any plasmonic nanostructures.

References

[1]   W. L. Barnes, A. Dereux, and T. W. Ebbesen, "Surface plasmon subwavelength optics," *Nature,* vol. 424, pp. 824-830, 2003.

[2]   S. A. Maier, *Plasmonics: fundamentals and applications*: Springer Science & Business Media, 2007.

[3]   D. K. Gramotnev and S. I. Bozhevolnyi, "Plasmonics beyond the diffraction limit," *Nature photonics,* vol. 4, pp. 83-91, 2010.

[4]   R. J. Blaikie and D. O. Melville, "Imaging through planar silver lenses in the optical near field," *Journal of Optics A: Pure and Applied Optics,* vol. 7, p. S176, 2005.

[5]   D. Melville and R. Blaikie, "Super-resolution imaging through a planar silver layer," *Optics Express,* vol. 13, pp. 2127-2134, 2005.

[6]   A. Hosseini and Y. Massoud, "A low-loss metal-insulator-metal plasmonic bragg reflector," *Optics express,* vol. 14, pp. 11318-11323, 2006.

[7]   A. J. Haes and R. P. Van Duyne, "A nanoscale optical biosensor: sensitivity and selectivity of an approach based on the localized surface plasmon resonance spectroscopy of triangular silver nanoparticles," *Journal of the American Chemical Society,* vol. 124, pp. 10596-10604, 2002.

[8]   J. Henzie, M. H. Lee, and T. W. Odom, "Multiscale patterning of plasmonic metamaterials," *Nature nanotechnology,* vol. 2, pp. 549-554, 2007.

[9]   V. E. Ferry, L. A. Sweatlock, D. Pacifici, and H. A. Atwater, "Plasmonic nanostructure design for efficient light coupling into solar cells," *Nano letters,* vol. 8, pp. 4391-4397, 2008.

[10]   S. Y. Chou and W. Ding, "Ultrathin, high-efficiency, broad-band, omni-acceptance, organic solar cells enhanced by plasmonic cavity with subwavelength hole array," *Optics express,* vol. 21, pp. A60-A76, 2013.

[11]   S. A. Maier, "Plasmonics: Metal nanostructures for subwavelength photonic devices," *Selected Topics in Quantum Electronics, IEEE Journal of,* vol. 12, pp. 1214-1220, 2006.

[12]   S. A. Maier, "Plasmonics: The promise of highly integrated optical devices," *Selected Topics in Quantum Electronics, IEEE Journal of,* vol. 12, pp. 1671-1677, 2006.

[13]   I. V. Shadrivov, V. A. Fedotov, D. A. Powell, Y. S. Kivshar, and N. I. Zheludev, "Electromagnetic wave analogue of an electronic diode," *New Journal of Physics,* vol. 13, p. 033025, 2011.

[14]   K. Gallo, G. Assanto, K. R. Parameswaran, and M. M. Fejer, "All-optical diode in a periodically poled lithium niobate waveguide," *Applied Physics Letters,* vol. 79, pp. 314-316, 2001.

[15]   M. Scalora, J. P. Dowling, C. M. Bowden, and M. J. Bloemer, "The photonic band edge optical diode," *Journal of Applied Physics,* vol. 76, pp. 2023-2026, 1994.

[16]   M. D. Tocci, M. J. Bloemer, M. Scalora, J. P. Dowling, and C. M. Bowden, "Thin-film nonlinear optical diode," *Applied physics letters,* vol. 66, pp. 2324-2326, 1995.

[17]   X.-S. Lin, J.-H. Yan, L.-J. Wu, and S. Lan, "High transmission contrast for single resonator based all-optical diodes with pump-assisting," *Optics express,* vol. 16, pp. 20949-20954, 2008.

[18]   H. Zhou, K.-F. Zhou, W. Hu, Q. Guo, S. Lan, X.-S. Lin*, et al.*, "All-optical diodes based on photonic crystal molecules consisting of nonlinear defect pairs," *Journal of applied physics,* vol. 99, p. 123111, 2006.

[19]   S. F. Mingaleev and Y. S. Kivshar, "Nonlinear transmission and light localization in photonic-crystal waveguides," *JOSA B,* vol. 19, pp. 2241-2249, 2002.

[20]   E. Verhagen, "Subwavelength light confinement with surface plasmon polaritons," 2009.

[21]   H. Raether, *Surface plasmons on smooth surfaces*: Springer, 1988.

[22]   A. Archambault, T. V. Teperik, F. Marquier, and J.-J. Greffet, "Surface plasmon Fourier optics," *Physical Review B,* vol. 79, p. 195414, 2009.

[23]   E. Jin and X. Xu, "Plasmonic effects in near-field optical transmission enhancement through a single bowtie-shaped aperture," *Applied Physics B,* vol. 84, pp. 3-9, 2006.

[24]   J. T. Krug II, E. J. Sánchez, and X. S. Xie, "Design of near-field optical probes with optimal field enhancement by finite difference time domain electromagnetic simulation," *The Journal of chemical physics,* vol. 116, pp. 10895-10901, 2002.

[25]   W. H. Pernice, F. P. Payne, and D. F. Gallagher, "A general framework for the finite-difference time-domain simulation of real metals," *Antennas and Propagation, IEEE Transactions on,* vol. 55, pp. 916-923, 2007.

[26]   A. D. Rakić, A. B. Djurišić, J. M. Elazar, and M. L. Majewski, "Optical properties of metallic films for vertical-cavity optoelectronic devices," *Applied optics,* vol. 37, pp. 5271-5283, 1998.

[27]   M. A. Ordal, R. J. Bell, R. Alexander, L. Long, and M. Querry, "Optical properties of fourteen metals in the infrared and far infrared: Al, Co, Cu, Au, Fe, Pb, Mo, Ni, Pd, Pt, Ag, Ti, V, and W," *Applied optics,* vol. 24, pp. 4493-4499, 1985.

[28]   G. Veronis and S. Fan, "Bends and splitters in metal-dielectric-metal subwavelength plasmonic waveguides," *Applied Physics Letters,* vol. 87, p. 131102, 2005.

[29]   H. Gao, H. Shi, C. Wang, C. Du, X. Luo, Q. Deng*, et al.*, "Surface plasmon polariton propagation and combination in Y-shaped metallic channels," *Optics express,* vol. 13, pp. 10795-10800, 2005.

[30]   B. Wang and G. P. Wang, "Surface plasmon polariton propagation in nanoscale metal gap waveguides," *Optics letters,* vol. 29, pp. 1992-1994, 2004.

[31]   G. Veronis and S. Fan, "Theoretical investigation of compact couplers between dielectric slab waveguides and two-dimensional metal-dielectric-metal plasmonic waveguides," *Optics Express,* vol. 15, pp. 1211-1221, 2007.

[32]   P. Ginzburg and M. Orenstein, "Plasmonic transmission lines: from micro to nano scale with λ/4 impedance matching," *Optics express,* vol. 15, pp. 6762-6767, 2007.

[33]   D. Pile and D. K. Gramotnev, "Adiabatic and nonadiabatic nanofocusing of plasmons by tapered gap plasmon waveguides," *Applied Physics Letters,* vol. 89, p. 041111, 2006.

[34]   R. Wahsheh, Z. Lu, and M. Abushagur, "Nanoplasmonic air-slot coupler: design and fabrication," in *Frontiers in optics*, 2012, p. FTh4A. 6.

[35]   R. Luebbers, F. P. Hunsberger, K. S. Kunz, R. B. Standler, and M. Schneider, "A frequencydependent finite-difference time-domain formulation for dispersive materials," Electromagnetic Compatibility, IEEE Transactions on, vol. 32, no. 3, pp. 222–227, 1990.

[36] D. F. Kelley and R. J. Luebbers, "Piecewise linear recursive convolution for dispersive media using fdtd," Antennas and Propagation, IEEE Transactions on, vol. 44, no. 6, pp. 792–797, 1996.

[37] R. J. Luebbers, F. Hunsberger, and K. S. Kunz, "A frequency-dependent finite-difference time-domain formulation for transient propagation in plasma," Antennas and Propagation, IEEE Transactions on, vol. 39, no. 1, pp. 29–34, 1991.

[38] R. J. Luebbers and F. Hunsberger, "Fdtd for¡ e1¿ n¡/e1¿ th-order dispersive media," Antennas and Propagation, IEEE Transactions on, vol. 40, no. 11, pp. 1297–1301, 1992.

[39] F. Hunsberger, R. Luebbers, and K. Kunz, "Finite-difference time-domain analysis of gyrotropic media. i. magnetized plasma," Antennas and Propagation, IEEE Transactions on, vol. 40, no. 12, pp. 1489–1495, 1992

[40] F. Hunsberger, R. Luebbers, and K. Kunz, "Finite-difference time-domain analysis of gyrotropic media. i. magnetized plasma," Antennas and Propagation, IEEE Transactions on, vol. 40, no. 12, pp. 1489–1495, 1992

[41] A. Akyurtlu and D. H. Werner, "Bi-fdtd: A novel finite-difference time-domain formulation for modeling wave propagation in bi-isotropic media," Antennas and Propagation, IEEE Transactions on, vol. 52, no. 2, pp. 416–425, 2004

[42] A. Grande, I. Barba, A. C. Cabeceira, J. Represa, P. P. So, and W. J. Hoefer, "Fdtd modeling of transient microwave signals in dispersive and lossy bi-isotropic media," Microwave Theory and Techniques, IEEE Transactions on, vol. 52, no. 3, pp. 773–784, 2004.

[43] A. Akyurtlu and D. H. Werner, "A novel dispersive fdtd formulation for modeling propagation in chiral metamaterials," Antennas and Propagation, IEEE Transactions on, vol. 52, no. 9, pp. 2267–2276, 2004